

DISSERTATION

**Numerical Modelling and Simulation for Flow Maldistribution in
Microtube Strip (MTS) Heat Exchanger**

by

Afiq Noor Bin Tuah

Dissertation submitted in partial fulfillment of
the requirements for the
Bachelor of Engineering (Hons)
(Chemical Engineering)

SEPTEMBER 2012

Universiti Teknologi PETRONAS

Bandar Seri Iskandar

31750 Tronoh

Perak Darul Ridzuan

CERTIFICATION OF APPROVAL

Numerical Modelling and Simulation for Flow Maldistribution in Microtube Strip (MTS) Heat Exchanger

by

Afiq Noor Bin Tuah

A project dissertation submitted to the
Chemical Engineering Programme
Universiti Teknologi PETRONAS
in partial fulfilment of the requirement for the
BACHELOR OF ENGINEERING (Hons)
(CHEMICAL ENGINEERING)

Approved by,

(Dr. Anis Suhaila Binti Shuib)

UNIVERSITI TEKNOLOGI PETRONAS
TRONOH, PERAK
September 2012

CERTIFICATION OF ORIGINALITY

This is to certify that I am responsible for the work submitted in this project, that the original work is my own except as specified in the references and acknowledgements, and that the original work contained herein have not been undertaken or done by unspecified sources or persons.

AFIQ NOOR BIN TUAH

ABSTRACT

Microtube Strip (MTS) heat exchanger is a laminar flow heat exchanger that consist of several numbers of small modules connected to each other in parallel. MTS heat exchanger proves to have higher efficiency and at the same time smaller than conventional turbulence flow heat exchanger. Hence, it is very suitable to be used as a cooling medium to remove the extra heat generated by F1 car engine. However, one of the problems in MTS heat exchanger is flow maldistribution whereby there is unequal distribution of fluid flow inside the heat exchanger which is due to poor header configuration. Thus, the objective of this project is to investigate the effect of different header configuration on flow maldistribution severity in MTS heat exchanger. For this project, two headers had been chosen for fluid flow simulation which is semi cylindrical header and pyramidal header. In order to simulate the fluid flow in both of the headers, CFD FLUENT had been used based on finite volume method. During the simulation, velocity distribution and temperature distribution data on outlet tubes had been obtained. The relative and absolute flow maldistribution parameter for both of the headers had been calculated by using the velocity distribution data while validation had been performed by comparing the temperature distribution data from simulation with the temperature data from experiment. As a conclusion, semi cylindrical header is 70 while for pyramidal header is 60. Hence, pyramidal header is relatively better than semi cylindrical header in term of reducing the severity of flow maldistribution. The reason is because of the geometry for pyramidal header had resulted a flow with less maldistribution compared to semi cylindrical header.

ACKNOWLEDGEMENT

In the Name of Allah, The Most Merciful and Compassionate, praise to Allah, He is the Almighty. Eternal blessings and peace upon the Glory of the Universe, our beloved Prophet Muhammad (S.A.W), his family and companions. First and foremost, thanks to the Almighty for the strength given to carry out the Plant Design Project I in September 2012 Semester. A deep gratitude goes for the my supportive families, who throughout the way provide them with motivation in completing the project.

Special regards with deepest appreciation dedicated to DR ANIS SUHAILA BINTI SHUIB, my beloved supervisor for her continuous support and help throughout the project consultation. The supervision and support that she gave truly help the progression and smoothness in completing the project.

This acknowledgement is extended to all other lecturers who continuously show their cooperation to the project. My gratitude also goes to the course mates in exchanging ideas and provides guidance in application of design and simulation software. Last but not the least, I would also like to show my heartfelt gratitude to all those who has directly or indirectly involved in this project, for their tremendous support and motivation during undertaking this project.

TABLE OF CONTENTS

CERTIFICATION OF APPROVAL	i
CERTIFICATION OF ORIGINALITY	ii
ABSTRACT.....	iii
ACKNOWLEDGEMENT.....	iv
CHAPTER 1: PROJECT BACKGROUND.....	1
1.1 Background of Study.....	1
1.2 Problem Statement.....	3
1.3 Objective	3
1.4 Scope of Study.....	3
1.5 Relevancy of Project.....	4
1.6 Feasibility of Project.....	4
CHAPTER 2: LITERATURE REVIEW.....	5
2.1 Micro Heat Exchanger.....	5
2.2 MTS Heat Exchanger.....	5
2.2.1 MTS Heat Exchanger Components.....	6
2.2.2 Theoretical Analysis.....	7
2.2.3 Experimental Analysis.....	10
2.3 Flow Maldistribution.....	11
CHAPTER 3: METHODOLOGY.....	13
3.1 Research Methodology.....	13
3.2 Project Activities.....	14
3.3 Tools/Method.....	15

	3.3.1 Geometry.....	16
	3.3.2 Mesh	18
	3.3.3 Physics	18
	3.3.4 Solve.....	19
	3.3.5 Report and Post-Processing.....	20
	3.4 Key Milestones.....	21
	3.5 Gantt Chart.....	22
CHAPTER 4:	RESULT AND DISCUSSION.....	23
	4.1 MTS Heat Exchanger Design.....	23
	4.2 Meshing.....	25
	4.3 Scaled Residual.....	27
	4.4 Mass Flow Report.....	28
	4.5 Velocity Distribution.....	29
	4.5.1 Semi Cylindrical Header.....	30
	4.5.2 Pyramidal Header	33
	4.6 Temperature Distribution.....	37
	4.6.1 Semi Cylindrical Header.....	37
	4.6.2 Pyramidal Header	38
	4.6 Discussion.....	40
	4.7.1 Comparison on Relative Flow Maldistribution Parameter	40
	4.7.2 Comparison on Temperature Distribution.....	41
	4.7.2 Validation.....	42
CHAPTER 5:	CONCLUSION AND RECOMMENDATION	44
	5.1 Conclusion.....	44

	5.2 Recommendation.....	44
CHAPTER 6:	REFERENCES.....	45

LIST OF FIGURES

Figure 1.1	Examples of header configuration for MTS heat exchanger	2
Figure 2.1	Microtube strip heat exchanger drawing	6
Figure 2.2	Binary branched constructal distributor	12
Figure 3.1	Research methodology	13
Figure 3.2	Process flow for CFD numerical modelling and simulation	15
Figure 4.1	Isometric drawing of one module of MTS heat exchanger	23
Figure 4.2	Cross sectional view of tube arrangement for MTS heat exchanger at the header	23
Figure 4.3	Isometric drawing of semi cylindrical header	24
Figure 4.4	Isometric drawing of pyramidal header	24
Figure 4.5	Semi cylindrical header that had been meshed	25
Figure 4.6	Pyramidal header that had been meshed	25
Figure 4.7	Scaled residual for semi cylindrical header fluid flow analysis	27
Figure 4.8	Scaled residual for pyramidal header fluid flow analysis	27
Figure 4.9	Contour of velocity at each of the outlet tubes for semi cylindrical header	30
Figure 4.10	Velocity vector for half section of semi cylindrical header	31
Figure 4.11	Velocity magnitude (m/s) vs. serial number of outlet tubes for semi cylindrical header	32
Figure 4.12	Relative flow maldistribution vs. serial number of outlet tubes for semi cylindrical header	33
Figure 4.13	Contour of velocity at each of the outlet tube for pyramidal header	34
Figure 4.14	Velocity vector for pyramidal header	34
Figure 4.15	Velocity magnitude (m/s) vs. serial number of outlet tubes for pyramidal header	35
Figure 4.16	Relative flow maldistribution vs. serial number of outlet tubes for pyramidal header	36

Figure 4.17	Contour for temperature (K) at each outlet tubes for semi cylindrical header	37
Figure 4.18	Temperature (K) vs. serial number of outlet tubes for semi cylindrical header	38
Figure 4.19	Contour for temperature (K) at each outlet tubes for pyramidal header	39
Figure 4.20	Temperature (K) vs. serial number of outlet tubes for pyramidal header	40
Figure 4.21	Comparison on relative flow maldistribution parameter between semi cylindrical header and pyramidal header	40
Figure 4.22	Comparison on temperature (K) between semi cylindrical header and pyramidal header	41

LIST OF TABLES

Table 2.1	Experimental and predicted heat transfer data	10
Table 3.1	Proposed project activities	14
Table 3.2	Analysis on header/distributor configuration	16
Table 3.3	Geometry for MTS heat exchanger	17
Table 3.4	Geometry for semi cylindrical and pyramidal header	17
Table 3.5	Parameter for physics step	18
Table 3.6	Parameter for solver step	19
Table 3.7	Parameter for report step	20
Table 3.8	Key milestone for project	21
Table 3.9	Proposed Gantt chart for project implementation	22
Table 4.1	Mesh Statistic for Semi Cylindrical Header	26
Table 4.2	Mesh Statistic for Pyramidal Header	26
Table 4.3	Mesh Statistic for Semi Cylindrical Header	29
Table 4.4	Experimental Data for a Complete Prototype of MTS Heat Exchanger	42

CHAPTER 1

PROJECT BACKGROUND

1.1 Background Of Study

Conventional designs of heat exchanger will focus on the designs that operate in turbulence flow regime in order to take advantage of the high heat transfer coefficient associated to turbulent flow. As a result, it will minimize the manufacturing and material costs of the heat exchanger. However, in terms of minimizing the work required to overcome fluid friction in the heat exchanger and also maximising the heat exchanger effectiveness, laminar flow heat exchanger is a better choice. This is because, a turbulent flow heat exchanger will result in higher penalty in pumping work and the vibration produced by the turbulence will decrease the life of the heat exchanger. Besides that, according to the second law of thermodynamic, in order to have a high efficiency heat exchanger, the flow must be laminar with a minimum temperature difference between counter flowing streams. Example of laminar flow heat exchangers is MTS heat exchanger which is a laminar flow heat exchanger that consist of several numbers of small modules connected to each other in parallel. In each module, there will be 8 rows of 40 to 200 microtubes with 0.8 mm outside diameter and 0.16 m length

Despite of all the advantages that laminar flow heat exchanger had offered, the difficulties in manufacturing the heat exchanger itself had made it not popular among the designer. This is because, in order to have a heat exchanger that works in a laminar flow, the tubes must be in micron size to ensure that the Reynold number will be small. As a result, the cost for manufacturing the laminar flow heat exchanger using conventional methods will be very expensive and impractical. However, with the availability of new technologies that involves advance manufacturing techniques such as diffusion welding and finebanking technology, the manufacturing cost had become cheaper and it will be possible to manufacture the laminar flow heat exchanger.

Basically, MTS heat exchanger will consist of many micro size tubes that are manifold together in parallel, with a surrounding cage to develop a counterflow condition. Even though crossflow is believe to simplify manifolding problem but in term of maximum practical effectiveness, a crossflow direction can only have a maximum of 80% effectiveness in a symmetric flow condition. Besides that, there is also an increase in pumping power loses due to the existence of turbulence. On the other hand, with a counterflow, it is practical to achieve 100% effectiveness under symmetric condition. Thus, counterflow had been chosen instead of crossflow for the laminar flow heat exchanger.

By taking advantage of the high efficiency MTS heat exchanger, there are suggestions that this heat exchanger can be applied in space-power application and closed cycle applications. Due to the small size and high efficiency, MTS heat exchanger is very suitable to be used as a cooling medium to remove extra heat generated by the formula one car engine.. However, there are several issues that must be taken into consideration when designing MTS heat exchanger which is flow maldistribution due to poor header configuration. Thus, careful design of header configuration is required in order to reduce the effect of flow maldistribution. Fig 1.1 shows examples of header configuration for MTS heat exchanger that can be used to reduce the effect of flow maldistribution.

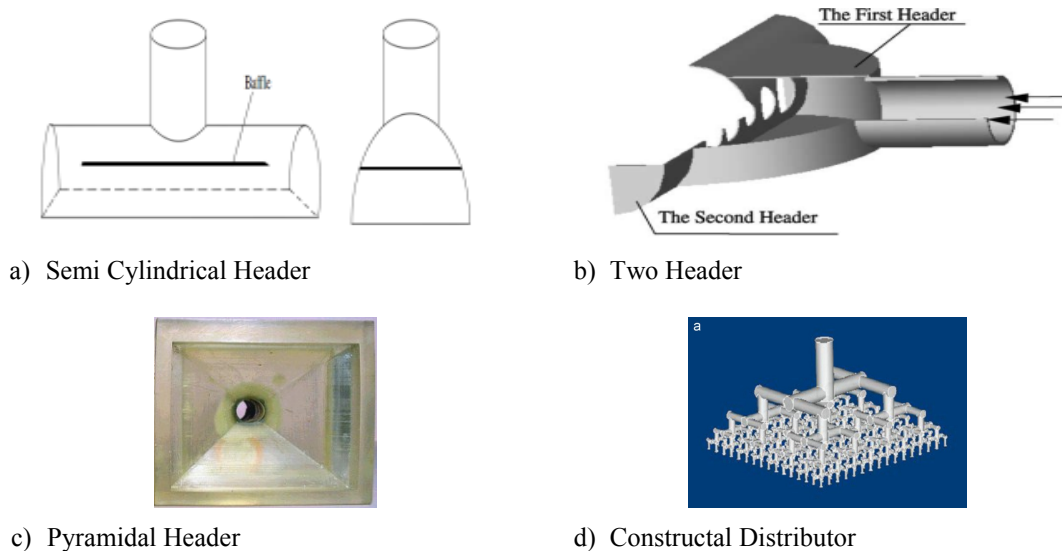


Figure 1.1: Examples of header configuration for MTS heat exchanger

1.2 Problem Statement

1.2.1 Problem Identification

Flow maldistribution is one of the problems in microtube strip heat exchanger, whereby the fluid flow and the heat are not being distributed uniformly inside the heat exchanger. As a result, the efficiency of a microtube strip heat exchanger will be reduced due to decreasing of heat transfer rate and increasing of pressure drop in the heat exchanger. One of the reasons for flow maldistribution is improper heat exchanger entrance configuration such as poor design of header and distributor configuration. Besides that, manufacturing tolerance, fouling, and frosting of condensable impurities are also the reasons for flow maldistribution.

1.2.2 Significant of the Project

This project will help to investigate the severity of flow maldistribution in microtube strip heat exchanger. Besides that, the analysis on the optimum design can help in decreasing the impact of flow maldistribution and thus increasing the performance of the heat exchanger.

1.3 Objective

The objective for this project is to investigate the effect of different header configuration on flow maldistribution severity in MTS heat exchanger.

1.4 Scope Of Studies

Analysis on MTS heat exchanger is being done using Computational Fluid Dynamic(CFD) simulation. However, due to software limitation, the Investigation of flow maldistribution is being done only on the inlet tube-side fluid in one module of MTS heat exchanger

1.5 Relevancy Of Project

In relevance to the course of study, this project requires the basic understanding of thermodynamic as well as heat exchanger design which is one of the core studies in chemical engineering programme. By doing this project, the student can learn to integrate theoretical knowledge into practical application which can help in further understanding on the subject matter. Besides that, this project will also involve computational fluid dynamic simulation on the micro heat exchanger using FLUENT software that is related to fluid dynamic subject. Here, fluid dynamic knowledge can be applied in designing the micro heat exchanger such as determining the type of flow and analysing heat distribution inside the micro heat exchanger.

1.6 Feasibility Of Project

Due to the limitation of time, it is not feasible to perform this project experimentally. However, with the help of computational fluid dynamic software such as FLUENT, it is feasible to perform a numerical simulation and modelling on the microtube strip heat exchanger. Besides that, the scope of the project had also been narrowed down into optimization of inlet distributor configuration to reduce the effect of flow maldistribution in the tube-side fluid flow only. This is to ensure that the project will be completed within the required time frame.

CHAPTER 2

LITERATURE REVIEW

2.1 Micro Heat Exchanger

There are many types of micro heat exchangers such as Counter Flow Micro Heat Exchanger (COMH), Laser Welded Micro Heat Exchanger and Brazed Micro Heat Exchanger. One of the common characteristics for all of these micro heat exchangers is that all of the micro heat exchangers will have at least one fluid flows in micro channels with a hydraulic diameter below 1 mm. Besides that, in order to obtain the micro channels with a hydraulic diameter below 1 mm, micro-structured plates had been used. These micro heat exchangers had a lot of advantageous compared to the macro-scale heat exchangers. One of the advantages is better performance by improving heat transfer coefficient with large number of smaller channels. Besides that, lower weight reduces the structural and support requirements. Other than that, in term of cost, it is much cheaper due to less materials being used during fabrication. Furthermore, since it small, it is more mobile than the macro-scale heat exchanger. However, due to the small hydraulic diameter, the efficiency of the micro heat exchanger is lower than the macro scale heat exchanger and there will be a significant pressure loss inside the micro heat exchanger.

2.2 MTS Heat Exchanger

In order to improve the efficiency of the micro heat exchanger, F. David Doty had come out with an ingenious solution by designing the micro heat exchanger using micro tube instead of the conventional micro-structured plate. This new approach of micro heat exchanger is called as Microtube Strip Heat Exchanger (MTS) whereby it consist of several numbers of small modules connected to each other in parallel. In each module, there will be 8 rows of 40 to 200 microtubes with 0.8 mm outside diameter and 0.16 m length [1].

2.2.1 MTS Heat Exchanger Components

Fig. 2.1a shows the drawing for a single MTS module while Fig. 2.1b shows the drawing for MTS modules that are manifolded together in parallel to form MTS block [1]

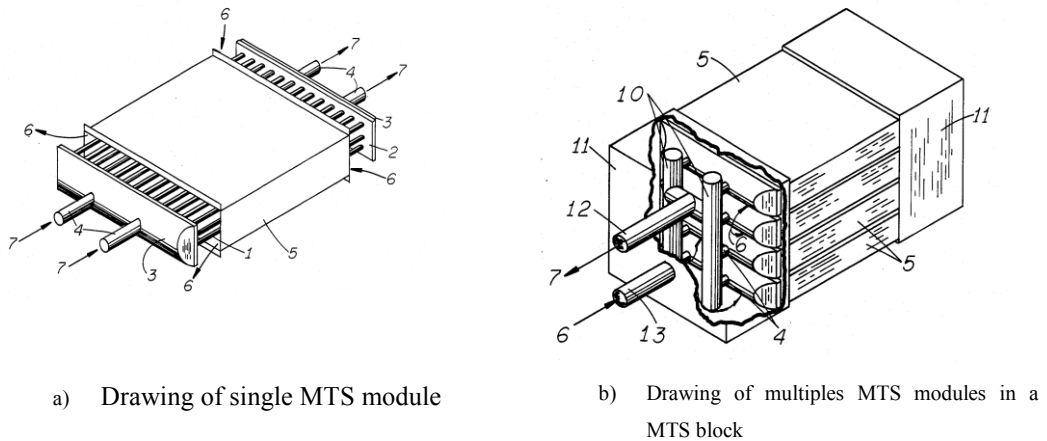


Figure 2.1: Microtube Strip Heat Exchanger Drawing

From Fig. 2.1a and Fig. 2.1b, a set of numbers from 1 to 13 can be seen whereby each of this numbers represent every parts inside the Microtube Strip Heat Exchanger. Number 1 is actually the microtubes that can be manufactured using high-speed laser welding technology and diamond dies at production cost as low as \$0.14 per meter [2]. These microtubes can be joined to the MTS header strip which is denoted by number 2 by a technique called diffusion welding whereby clean metal surfaces are held together under pressure at high temperature [3]. Due to the combined effect of solid-state surface tension and solid-state diffusion mechanism, there will be migration of atoms across the join which result in recrystallization. The time required to form the bond is an inverse exponential function of temperature and a quadratic function of surface finish and interfacial gaps [3]. In the case of MTS heat exchanger, about 10 s at 1230 °C is required for full strength diffusion welds in the Ni-Cr-W superalloy [2]. In order to achieve a good result with 100% leak-tight on the surface, the surface finishes must be about 0.4 μm rms in the area of the diffusion weld [2]. Besides that, before assembling, the tubes and holes on the header strip must be thoroughly cleaned without any oxide. Other than that, the interference press fit must be maintained at a minimum of 0.3% [1].

On the header strip, there will be an equivalent amount of holes for each of the microtubes. However, since it will require very small hole to accommodate the microtubes, conventional method will not be sufficient. Hence, Swiss finebanking technology had been used to make the required hole on the header strip. This technology is actually a controlled cold-flow punching process whereby a counterpunch and high pressure ring indenter will apply sufficient pressure to the metal surfaces near the punch edges [4]. By doing this, the required hole diameter with a tolerance of $\pm 0.9\%$ can be obtained without any normal and planar deformation of the material during punching [2]. Number 3 is the semi-cylindrical cap that had been welded to each of the header strips while number 4 is the tube side manifold ports that are provided on each cap. In order to force the shell-side fluid to enter the periphery of the MTS sub-assembly at one end and exit in similar manner at the other end, a cage denoted by number 5 had been put closely surrounds the MTS sub-assembly, except near each of the header strip. The flow for the shell-side fluid is being represented by number 6. On the other hand, the tube-side fluid which is denoted by number 7 will enters the tube-side manifold ports in a counter flow direction to the shell-side fluid.

As for the MTS block that consists of several MTS modules being manifold together in parallel, the individual tube-side manifold port will be connected to the block tube-side manifold at each end which is denoted by number 10. The block cage which is denoted by number 11 will form the shell-side region together with the MTS module cage. For the flow of the fluid, the tube-side fluid may flow through the tube-side block port which is denoted by number 12. On the other hand, the shell-side fluid may flow in the opposite direction through the shell-side block port which is denoted by number 13.

2.2.2 Theoretical Analysis

In order to evaluate the performance of a heat exchanger, efficiency is always being used. This is because, efficiency is actually the ratio of actual heat transfer rate in a heat exchanger to the thermodynamically limited maximum possible heat transfer rate that can be transferred by a heat exchanger having infinite surface area and operating under the same pressure [5]. In the case of MTS heat exchanger which is

basically a counter flow heat exchanger, the effectiveness is given by the following equation

$$\epsilon = \frac{1 - e^{-NTU(1-R)}}{1 - e^{-NTU(1-R)R}} \quad (1)$$

Where NTU is the number of transfer unit and is given by the following equation:

$$NTU = \frac{UA}{c\dot{m}} \quad (2)$$

c and \dot{m} are the specific heat and mass flow rate of the fluid stream that have less heat capacity respectively. On the other hand, R is the ratio of the lesser heat capacity to the greater and is being expressed as:

$$R = \frac{c_{\min}\dot{m}_{\min}}{c_{\max}\dot{m}_{\max}} \quad (3)$$

For two streams with equal capacities, Eq. 1 will become undefined and can be replaced by a simpler expression:

$$\epsilon = \frac{NTU}{NTU + 1} \quad (4)$$

MTS heat exchanger is considered to be a tubular counterflow heat exchanger made up of n tubes, length L , internal diameter d_i with laminar flow inside and outside. Besides that, fluid flowing within the tubes is hotter on the entry and the conductivity of the tube material is large compared with that of the two fluids [2]. Thus, the term UA from Eq. 2 can be expressed as:

$$UA = 4\pi nL \left(\frac{k_c k_H}{ak_c + bk_H} \right) \quad (5)$$

Where k_H and k_C are the thermal conductivities of the inner and outer gases respectively while a and b are dimensionless coefficients of the order of unity that are functions of tube spacing, tube outer and inner diameters. So, for the geometric relationship, by assuming the tube centre spaced by $2d_i$ with tube wall equal to $0.2d_i$, a is approximately 0.7 while b is unity.

Similar like any other heat exchanger, there will be some factors that every designer will be concerned which are pumping losses, conduction losses, and cost of heat

exchanger. In term of cost for heat exchanger, it can be expressed as the mass of material required which is given as follows:

$$M = 0.24\pi d_i^2 n L \rho_m \quad (6)$$

As for the pumping power loss, \dot{W}_p it can be expressed as follows:

$$\dot{W}_p = \frac{128\mu L}{n\pi d_i^4} \left(\frac{\dot{m}_H}{\rho} \right)^2 \quad (7)$$

On the other hand, the conduction losses, \dot{W}_m through the tube metal from the hot end to the cool end can be expressed as follows:

$$\dot{W}_m \approx \frac{0.2n\pi d_i^2 k_m (T_H - T_C)}{L} \quad (8)$$

Where k_m is the tube metal conductivity while T_H and T_C are hot and cold temperature. In order to make sure that the internal flow is laminar, the following equation had been used

$$\text{Re} = \frac{4\dot{m}_h}{n\pi d_i \mu} \leq 2300 \quad (9)$$

Hence, by taking into consideration Eq. 1 until Eq. 9, a new ways of reducing the system mass had been developed which is by reducing d_i by a factor p , increasing n and decreasing L each by a factor p^2 [2]. Thus, the flow losses and UA terms will be constant which will result in a constant ϵ . In term of material cost, according to Eq. 6, mass will also be reduced by p^2 and hence, the cost will also be reduced by the same amount. In order to determine the lower limit on the tube diameter that will minimize pumping power losses and conduction losses a new equation had been derived which is given as follows [2].

$$d_i \geq \sqrt{\frac{20 \times 12,800\mu k_m}{\rho^2 c^2 (T_H - T_C)}} \quad (10)$$

For Eq. 10, a condition whereby both the pumping power and conduction losses may not exceed 1% of the ideal heat exchanger had been considered [2]. By evaluating Eq. 10, for a stainless steel heat exchanger with helium at 1 MPa as the process fluid, that has T_H equal to 900K while T_C equal to 300K, a lower limit on tube diameter of about 90 μm will be obtained. This lower limit on tube diameter had suggested that in order to minimize pumping power losses and conduction losses, it is desirable to design the smallest diameter tubes feasible in term of manufacturing and cost [2].

2.2.3 Experimental Analysis

In order to clarify his theoretical analysis, an experiment had been conducted. The objective of this experiment is to compare the experimental result on efficiency with the theoretical analysis [2]. For this experiment, several 103-tube MTS modules whereby each of the modules consists of 0.33 mm d_i tubes, 127 mm in length and 0.1524 mm walls [2]. Besides that, there are five rows of tubes with 21 holes in the odd-numbered rows and 20 holes in the even-numbered rows which had been arranged in a triangular pitch on 1.25 mm centre. In this experiment, three modules had been manifold together in parallel to distribute the tube-side and shell-side fluid flows. Other than that, there are also baffles installed between the modules to ensure uniform shell-side flow through each module [2].

Two gases had been selected for this experiment which is helium and nitrogen and in this experiment, the same fluid had been used for both tube-side and shell-side. Thus, the heat capacities are the same in both shell-side and tube-side. Table 1 shows the experimental and predicted heat transfer data [2].

Table 2.1: Experimental and Predicted Heat Transfer Data

\dot{m} (mg/s)	p (kPa)	T_1 (C)	T_2 (C)	T_3 (C)	T_4 (C)	ϵ (%)	NTU	UA (W/K)	UA [Eq. (5)]
Nitrogen									
470 ± 20	322 ± 3	104.7 ± 0.5	30.9 ± 0.5	23.0 ± 0.5	93.0 ± 0.5	85.7 ± 0.6	6.0 ± 0.3	3.7 ± 0.4	7.1
840 ± 20	322 ± 3	96.5 ± 0.5	32.3 ± 0.4	23.3 ± 0.5	84.1 ± 0.5	83.1 ± 0.7	4.9 ± 0.2	5.3 ± 0.5	7.1
930 ± 20	322 ± 3	99.4 ± 0.5	33.0 ± 0.5	22.8 ± 0.5	85.8 ± 0.5	8.2 ± 0.7	4.6 ± 0.2	5.4 ± 0.5	7.1
373 ± 20	705 ± 3	51.4 ± 0.5	28.5 ± 0.5	26.1 ± 0.5	48.8 ± 0.5	89.7 ± 0.7	8.7 ± 0.6	3.5 ± 1.4	7.1
738 ± 20	1462 ± 3	64.7 ± 0.5	28.9 ± 0.5	25.3 ± 0.5	59.2 ± 0.5	86.0 ± 0.7	6.1 ± 0.4	6.0 ± 1.3	7.1
1085 ± 20	1068 ± 3	64.8 ± 0.5	28.6 ± 0.5	23.6 ± 0.5	58.3 ± 0.5	84.2 ± 0.7	5.3 ± 0.3	7.1 ± 1.2	7.1
1413 ± 20	1486 ± 3	67.3 ± 0.5	29.3 ± 0.5	22.9 ± 0.5	59.5 ± 0.5	82.4 ± 0.7	4.7 ± 0.2	7.9 ± 1.1	7.1
1824 ± 20	1470 ± 3	58.1 ± 0.5	23.3 ± 0.5	15.3 ± 0.5	48.8 ± 0.5	78.2 ± 0.7	3.6 ± 0.1	7.6 ± 0.9	7.1
Helium									
117 ± 7	749 ± 3	107.5 ± 0.5	28.3 ± 0.5	23.5 ± 0.5	103.6 ± 0.5	95.4 ± 0.6	21 ± 3	11.1 ± 2.5	39.0
79 ± 7	756 ± 3	103.8 ± 0.5	29.5 ± 0.5	24.0 ± 0.5	100.5 ± 0.5	95.7 ± 0.7	22 ± 4	6.9 ± 1.6	39.0
213 ± 7	825 ± 3	109.4 ± 0.5	28.7 ± 0.5	23.1 ± 0.5	103.4 ± 0.5	93.0 ± 0.7	13.3 ± 1.4	15.4 ± 2.6	39.0

From table 2.1, there are few parameters that need to be clarified. First of all, T_1 and T_2 are the shell side inlet and outlet temperature respectively. On the other hand, T_3 and T_4 are the tube side inlet and outlet temperature respectively. Besides that, the first UA term is the experimental value of UA that is calculated using the following equation [2].

$$UA = \frac{\dot{m}c_p \Delta T}{T_s} \quad (11)$$

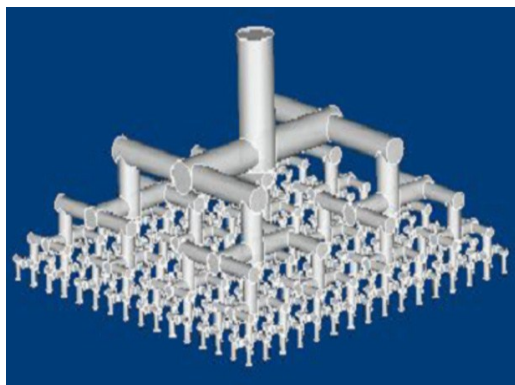
Where ΔT is the temperature difference between T_1 and T_2 while T_δ is the mean temperature difference between hot and cold streams. On the other hand, the second UA term is the theoretical value being calculated from Eq. 5. From the data in Table 1, it can be concluded that, the value of UA obtained by experimental data agree quite well with the theoretical value but only for effectiveness ranging from 75-85%. However, it is not the same with higher value of effectiveness whereby the experimental value of UA had deviate away from the theoretical value [2]. This might be due to flow maldistribution and the findings that the deviation from theoretical value is more serious at low flow rate support this reasoning [2].

2.3 Flow Maldistribution

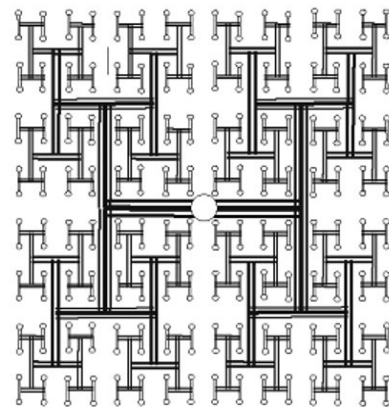
Hence, in order to increase the performance of the MTS heat exchanger, the flow maldistribution problem must be tackled and this is proven by a lot of research work on flow maldistribution such as by Mueller and Chiou [6]. Basically, flow maldistribution is unequal or non-uniform distribution of fluid or temperature throughout the heat exchanger [6]. There are two types of flow maldistribution which are passage-to-passage maldistribution and gross maldistribution [7]. The passage-to-passage maldistribution happens due to its manufacturing tolerance, fouling, and frosting of condensable impurities [7]. On the other hand, gross maldistribution is cause by improper heat exchanger entrance configuration such poor design of header and distributor configuration [7]. Since it is easier to reduce the effect of gross maldistribution by optimizing the heat exchanger design, more and more studies had been conducted on gross maldistribution instead of passage-to-passage maldistribution.

So, it is very important to optimize the design of the distributor and header by taking into account some properties which are equidistribution of the flow rate, minimal dispersion, minimal void volume, and minimal pressure drop. Hence, there had been several studies that had been done on improvement of distributor configuration to enhance the flow uniformity in heat exchanger. One of the suggestions is to use a perforated grid that can improve the fluid flow distribution [8]. Other than that, there is also other suggestion which is to add a second header for the heat exchanger inlet [9]. However, both of these solutions are not feasible in MTS heat exchanger since

MTS heat exchanger is more towards shell and tube heat exchanger than plate-fin heat exchanger. Furthermore, both of these solutions will also result in a higher pressure drop and flow dispersion that is undesirable from the engineering perspective. Another option of distributor is constructal distributor that is based from multi-scale optimization methodology known as constructal approach developed by Bejan [10]. Fig. 2.2a and Fig. 2.2b shows an example on binary branch of the construtal distributor pore structure and projection of pore network on base plane respectively [7]



a) Pore structure



b) Projection of pore network on base plane

Figure 2.2: Binary branched constructal distributor

In my opinion, constructal distributor is a better choice in reducing the effect of gross maldistribution in MTS heat exchanger due to the large number of tubes especially when there are many MTS modules being manifold together to form MTS block. The presences of levels of branching or also known as “generations” enable the fluid to be distributed uniformly in each of the tube and also shells. The number of level of branching will determine the number of final outlet which is given as 2^m , whereby m is the number of levels of branching [7]. However, due to the strong influence of internal structure, sudden changes of direction and sudden expansion or contractions along the tubes, there will be significant pressure drop for this distributor configuration which will result in higher pumping requirement. Hence, there is a need to find an optimum balance between pressure loss and flow uniformity.

CHAPTER 3

METHODOLOGY

3.1 Research Methodology

The methodology for this project started with project scope validation, project introduction, identifying and selection of possible header configuration, identifying and selection of CFD simulation software, conceptual design, detailed design, modelling and simulation, analysis of data, conclusion and finally recommendation.

Fig. 3.1 shows the research methodology for the project

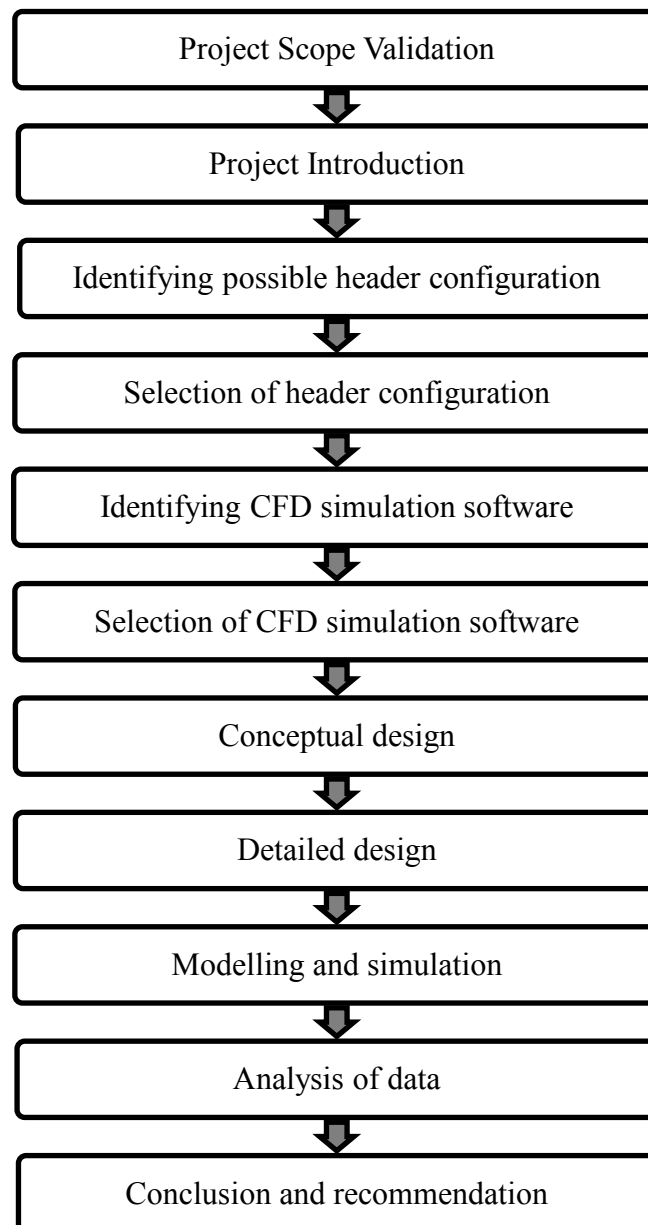


Figure 3.1: Research methodology

3.2 Project Activities

Table 3.1: Proposed Project Activities

Methodology	Activities
Project scope validation	<ul style="list-style-type: none"> • Confirmation of project title with supervisor • Problem statement identification • Scope of study identification
Project introduction	<ul style="list-style-type: none"> • Understanding the principle of heat exchanger design • Understanding the theory of microtube strip heat exchanger • Understanding the different types and factors that contribute to flow maldistribution in heat exchanger • Understanding different distributor configuration that can help reducing the effect of flow maldistribution
Identifying and selection of distributor configuration	<ul style="list-style-type: none"> • Feasibilities study on each of the distributor configuration
Identifying and selection of CFD simulation software	<ul style="list-style-type: none"> • Feasibilities study on each of the CFD simulation software
Conceptual design	<ul style="list-style-type: none"> • Preliminary design on MTS heat exchanger • Preliminary design on distributor configuration
Detailed design	<ul style="list-style-type: none"> • Determine the dimension for MTS heat exchanger • Determine the tube-side and shell side fluid • Determine the assembly and dimension for the distributor • Drawing the MTS heat exchanger using CAD software
Modelling and simulation	<ul style="list-style-type: none"> • Importing the geometry from CAD to CFD simulation software • Mesh • Specifying necessary parameters for the CFD simulation • Perform CFD simulation on MTS heat exchanger
Analysis of data	<ul style="list-style-type: none"> • Determine the velocity distribution at outlet tube • Calculate flow maldistribution parameter • Determine temperature distribution at outlet tube • Determine the vector of the fluid flow inside the MTS heat exchanger
Conclusion and recommendation	<ul style="list-style-type: none"> • Optimization of MTS heat exchanger design that can decrease the effect of flow maldistribution

Table 3.1 shows the proposed activities that will be conducted during the progress of the project.

3.3 Tools / Method

This project will use Computer Aided Design (CAD) software for designing and Computational Fluid Dynamic (CFD) software to perform simulation based on numerical modelling. CFD is the simulation of fluids engineering systems using mathematical physical problem formulation and numerical methods such as discretization methods, numerical parameters and grid generations. CFD need to be used for this project because it is more cost effective and time efficient in measuring the thermal performance of the MTS heat exchanger. Besides that, it is also easier to simulate the fluid flow using CFD rather than experiment.

There are a lot of codes for CFD such as commercial CFD code (FLUENT, star-CD, and CFX), research CFD code (CFDSHIP-IOWA) and public domain software (WinpipeD). Each of these codes will have different purposes to serve different applications. For this project a code is needed to analyse the flow maldistribution inside the MTS heat exchanger and in this case, either FLUENT or CFX can be used. Both of these codes were developed independently and have some common things whereby both are control-volume based for high accuracy and rely heavily on a pressure-based solution technique for broad applicability. However, there are significant differences between both of the codes in term of fluid flow equations integration and equation solution strategies. The CFX solver uses finite elements which is cell vertex numeric while the FLUENT solver uses a finite volume which is cell centred numeric. Besides that, CFX code focuses on one approach to solve the governing equations of motion (coupled algebraic multigrid), while the FLUENT codes offers several solution approaches (density, segregated, and coupled-pressure-based methods). Hence, based on the differences, FLUENT had been selected because it offers several solution approaches that can help in analysing the effect of flow maldistribution on the thermal performance of MTS heat exchanger.

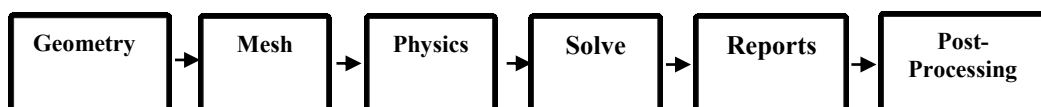


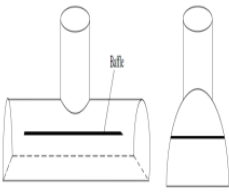
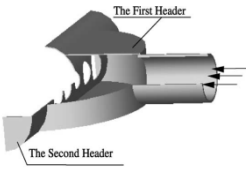
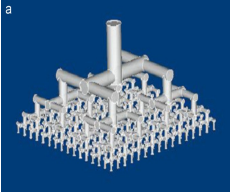
Figure 3.2: Process flow for CFD numerical modelling and simulation

Figure 3.2 shows the process flow that need to be conducted for the CFD numerical modelling and simulation

3.3.1 Geometry

In order to define the geometry for the MTS heat exchanger, CATIA had been selected as the design software. As for the header configuration, 4 header configurations had been identified which are baffle with small holes, two header, pyramidal distributor, and constructal distributor. Table 3.2 shows the analysis on different header/distributor configuration

Table 3.2: Analysis on Header/Distributor Configuration

Header/Distributor	Design	Advantages	Disadvantages
Baffle with small hole	 A technical drawing showing a cylindrical baffle with a central vertical tube. The baffle has a series of small holes along its length. The drawing includes a perspective view and a cross-sectional view.	<ul style="list-style-type: none"> • Uniform fluid velocity distribution • Cheap and convenient 	<ul style="list-style-type: none"> • Increase in pressure drop • Flow dispersion
Two header	 A 3D CAD model of a cylindrical header with two inlet/outlet ports. The top port is labeled 'The First Header' and the bottom port is labeled 'The Second Header'. The header has a series of small holes along its length.	<ul style="list-style-type: none"> • Uniform fluid velocity distribution • Cheap and convenient 	<ul style="list-style-type: none"> • Increase in pressure drop • Flow dispersion
Pyramidal distributor	 A photograph of a square pyramidal distributor. It is a square plate with a central circular hole and a series of smaller holes arranged in a grid pattern.	<ul style="list-style-type: none"> • Cheap and convenient • Uniform fluid velocity distribution 	<ul style="list-style-type: none"> • Increase in pressure drop
Constructal distributor	 A 3D CAD model of a constructal distributor. It is a complex, multi-tiered structure with a central vertical tube and a series of smaller tubes branching out from it, forming a tree-like structure.	<ul style="list-style-type: none"> • Uniform fluid velocity distribution • Lower pressure drop 	<ul style="list-style-type: none"> • Complex

Based on Table 3.2, ideally, constructal distributor seems to be the best choice. However, due to the complexity in its structure, it will not be feasible to design and at the same time conduct a simulation on the distributor within the given period of time. Hence, pyramidal distributor had been selected as the distributor configuration for MTS heat exchanger. This is because, the design is more simple than constructal distributal which make it feasible for the modelling and simulation phase. Besides that, unlike baffle with small hole and two header configuration, pyramidal distribution does not have a problem with flow dispersion. Geometry for the MTS heat exchanger and header configuration had been selected based on literature study. Table 3.3 and Table 3.4 show the geometry for MTS heat exchanger and pyramidal distributor respectively.

Table 3.3: Geometry for MTS Heat Exchanger

Parameter	Description
Tube inner diameter	0.33 mm
Tube length	127 mm
Distance between tube centers	1.25 mm
No. of rows	5 rows
Distance between rows	1.08 mm
No. of tubes	21 holes in odd number rows 20 holes in even number rows
Tubes arrangement	Triangular pitch

Table 3.4: Geometry for Semi Cylindrical Header and Pyramidal Header

Parameter	Description
Header length	27.5 mm
Header wide	6.82 mm
Inlet tube diameter	1 mm
Semi cylindrical header	Inner diameter : 6.82 mm No. of inlet tube : 2 Distance between tube : 9.17 mm
Pyramidal header	Inclination : 45° Height : 13.75 mm No of inlet tube : 1

3.3.2 Mesh

In mesh process, it must be well designed to resolve important flow features which are dependent upon flow condition parameters, such as the grid refinement inside the wall boundary layer. For this project, default parameters based on FLUENT as the solver preference had been set for the meshing process. In order to ensure that the geometry had been mesh correctly, the minimum value for the orthogonal quality of the mesh must not be less than 0.05 and the maximum value for skewness must not be greater than 0.90

3.3.3 Physics

In physics process, parameters like shell side fluid, tube side fluid, fluid type, boundary condition and initial condition. Table 3.5 shows the parameter for physics step.

Table 3.5: Parameter for Physics Step

Parameter	Description
Energy model	Energy equation
Viscous model	Standard k-epsilon model with enhanced wall treatment
Tube side fluid	Nitrogen
Boundary condition	Inlet : Mass flow inlet Outlet : pressure outlet Wall : Stationary and no slip
Initial condition	Wall temperature : 300K Inlet tube side temperature: 297K Inlet mass flow rate: 0.001 kg/s

3.3.4 Solve

In the solve process, the solver will solve the simulation based on the Navier-Stokes equation whereby since this project involve cylindrical coordinates, the following momentum equations for radius (r), diameter (ϕ), and gravity (z) will be used.

$$r: \rho \left(\frac{\partial u_r}{\partial t} + u_r \frac{\partial u_r}{\partial r} + \frac{u_\phi}{r} \frac{\partial u_r}{\partial \phi} + u_z \frac{\partial u_r}{\partial z} - \frac{u_\phi^2}{r} \right) = -\frac{\partial p}{\partial r} + \mu \left[\frac{1}{r} \frac{\partial}{\partial r} \left(r \frac{\partial u_r}{\partial r} \right) + \frac{1}{r^2} \frac{\partial^2 u_r}{\partial \phi^2} + \frac{\partial^2 u_r}{\partial z^2} - \frac{u_r}{r^2} - \frac{2}{r^2} \frac{\partial u_\phi}{\partial \phi} \right] + \rho g_r \quad (12)$$

$$\phi: \rho \left(\frac{\partial u_\phi}{\partial t} + u_r \frac{\partial u_\phi}{\partial r} + \frac{u_\phi}{r} \frac{\partial u_\phi}{\partial \phi} + u_z \frac{\partial u_\phi}{\partial z} + \frac{u_r u_\phi}{r} \right) = -\frac{1}{r} \frac{\partial p}{\partial \phi} + \mu \left[\frac{1}{r} \frac{\partial}{\partial r} \left(r \frac{\partial u_\phi}{\partial r} \right) + \frac{1}{r^2} \frac{\partial^2 u_\phi}{\partial \phi^2} + \frac{\partial^2 u_\phi}{\partial z^2} + \frac{2}{r^2} \frac{\partial u_r}{\partial \phi} - \frac{u_\phi}{r^2} \right] + \rho g_\phi \quad (13)$$

$$z: \rho \left(\frac{\partial u_z}{\partial t} + u_r \frac{\partial u_z}{\partial r} + \frac{u_\phi}{r} \frac{\partial u_z}{\partial \phi} + u_z \frac{\partial u_z}{\partial z} \right) = -\frac{\partial p}{\partial z} + \mu \left[\frac{1}{r} \frac{\partial}{\partial r} \left(r \frac{\partial u_z}{\partial r} \right) + \frac{1}{r^2} \frac{\partial^2 u_z}{\partial \phi^2} + \frac{\partial^2 u_z}{\partial z^2} \right] + \rho g_z. \quad (14)$$

Eq. 12, 13 and 14 are the momentum equation for radius (r), diameter (ϕ), and gravity (z) and it can be expressed using continuity equation as shown in Eq. 15

$$\frac{\partial \rho}{\partial t} + \frac{1}{r} \frac{\partial}{\partial r} (\rho r u_r) + \frac{1}{r} \frac{\partial (\rho u_\phi)}{\partial \phi} + \frac{\partial (\rho u_z)}{\partial z} = 0. \quad (15)$$

Besides that, appropriate numerical parameters and solvers must be setup for this step. Table 3.6 shows the parameter for the solver step.

Table 3.6: Parameter for Solver Step

Parameter	Description
Solver	<ul style="list-style-type: none"> • SIMPLE scheme for pressure-velocity coupling
Numerical scheme	<ul style="list-style-type: none"> • Second order discretization scheme
Convergent limit	<ul style="list-style-type: none"> • -3
Type of flow	<ul style="list-style-type: none"> • Steady state

3.3.5 Report and Post-Processing

In the report process, the time history of velocity residual, pressure and temperature can be saved. Besides that, integral quantities such as total pressure drop can be obtained and these data can be plotted in the XY graph. Table 3.7 shows the parameter for the report process

Table 3.7: Parameter for Report Step

Parameter	Description
XY plot	<ul style="list-style-type: none"> • Velocity Vs. Serial number of outlet tubes • Temperature Vs. Serial number of outlet tubes
Relative flow maldistribution parameter, S_i	$S_i = \frac{v_{ch(i)} - v_{ave}}{v_{ave}}$ Vch(i) : Velocity in each tube Vave : Average velocity
Absolute flow maldistribution parameter, S	$S = \sqrt{\frac{1}{N-1} \sum_{i=1}^N (v_{ch(i)} - v_{ave})^2}$ Vch(i) : Velocity in each tube Vave : Average velocity N : Number of tube

Finally, in post-processing, profile of temperature distribution, velocity distribution and pressure distribution will be collected.

3.4 Key Milestone

Table 3.8: Key Milestone for Project

Week	Objectives
FYP I	
5	Completion of preliminary research work
6	Submission of extended proposal
9	Completion of proposal defence
12	Confirmation on CFD simulation software
13	Submission of Interim draft report
14	Submission of Interim report
FYP II	
5	Finalized the design for micro heat exchanger
8	Submission of progress report
9	Completion of modelling and simulation
11	Pre-SEDEX
12	Submission of draft report
13	Submission of technical paper and dissertation
14	Oral presentation
15	Submission of project dissertation

Table 3.8 shows the key milestone for the project which is the objective that must be achieved within the specified week.

3.5 Gantt Chart

Table 3.9: Proposed Gantt Chart for Project Implementation

WEEK	FYPI														FYPII														
	1	2	3	4	5	6	7	8	9	10	11	12	13	14	1	2	3	4	5	6	7	8	9	10	11	12	13	14	15
Activities																													
1.0 Project Scope Validation	■	■																											
2.0 Project Introduction		■	■	■	■																								
3.0 Submission of Extended Proposal						■	■																						
4.0 Identifying and Selection of Possible Distributor Configuration						■	■	■																					
5.0 Identifying and Selection of CFD Simulation Softwares						■	■	■	■																				
6.0 Proposal Defence									■																				
7.0 Submission of Interim Draft Report												■																	
8.0 Submission of Interim Report												■																	
9.0 Conceptual Design									■	■	■	■	■	■															
10.0 Detailed Design															■	■													
11.0 Modelling and Simulation																■	■	■	■	■	■	■	■	■					
12.0 Analysis of Data																					■	■	■	■	■				
13.0 Submission of Progress Report																						■							
14.0 Conclusion and Recommendation																								■	■				
15.0 Pre-SEDEX																									■				
16.0 Submission of Draft Report																										■			
17.0 Submission of Technical Paper and Dissertation																											■		
18.0 Oral Presentation																												■	
19.0 Submission of Project Dissertation																												■	

Table 3.9 shows the proposed Gantt chart for the project implementation for both FYP I and FYP II. Based on the Gantt chart, the project is feasible to be completed within the given amount of time.

CHAPTER 4

RESULT AND DISCUSSION

4.1 MTS Heat Exchanger Design

Fig. 4.1 shows the isometric drawing of one module of MTS heat exchanger along with the geometry. On the other hand, Fig. 4.2 shows the tube arrangement for the MTS heat exchanger at the header.

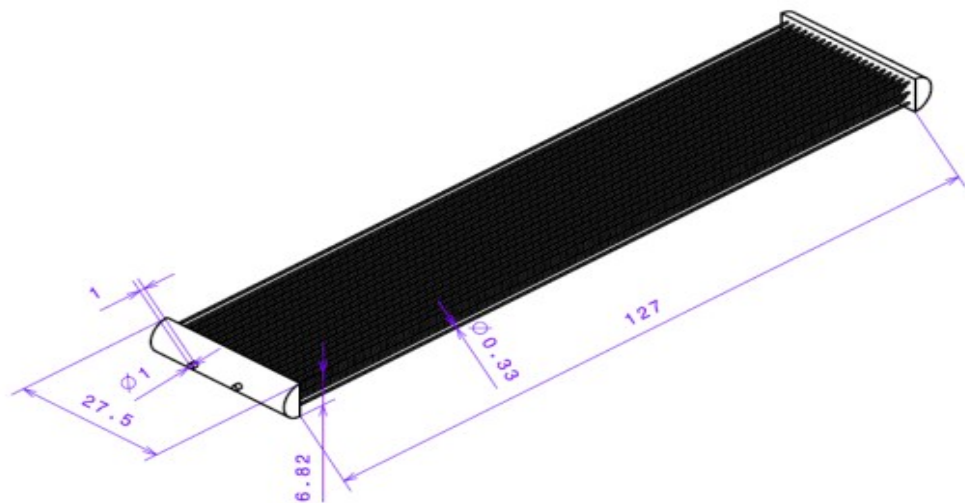


Figure 4.1: Isometric drawing of one module of MTS heat exchanger (Units in mm)

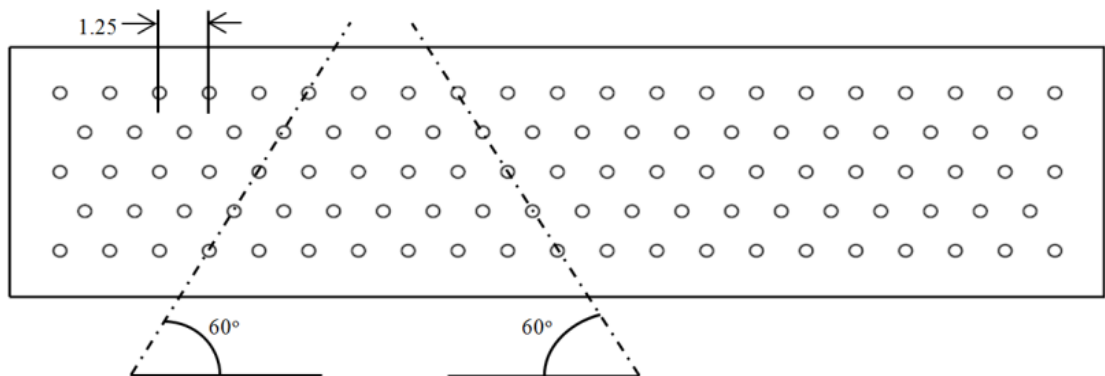


Figure 4.2: Cross sectional view of tube arrangement for MTS heat exchanger at the header

However, due to the complexity of the geometry, the meshing time will be too long and the software will not be able to mesh the geometry completely. Hence, the geometry needs to be simplified whereby, only the inlet header of the MTS heat exchanger will be used for the CFD simulation instead of the complete module of the MTS heat exchanger. As had been mentioned, there will be two headers that are

going to be analysed which are semi cylindrical and pyramidal. Fig. 4.3 and Fig. 4.4 show the isometric drawing for the semi cylindrical header and pyramidal header respectively that had been used in the fluid flow simulation using FLUENT.

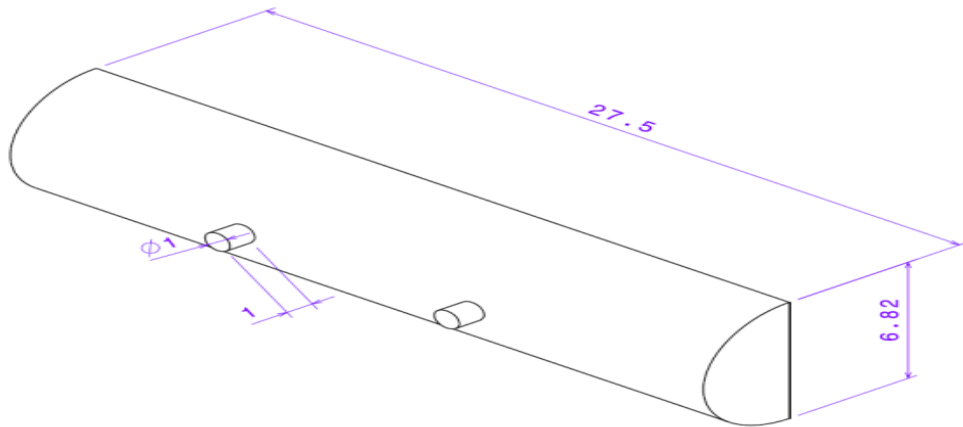


Figure 4.3: Isometric drawing of semi cylindrical header

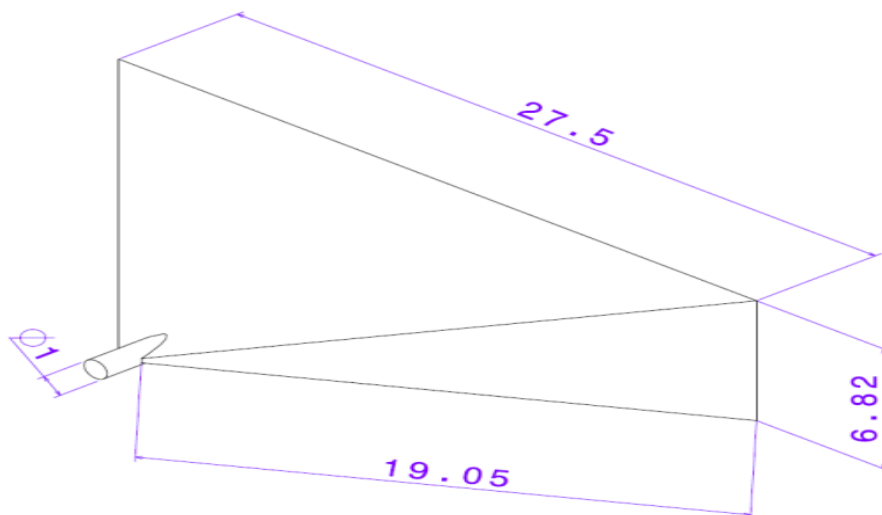


Figure 4.4: Isometric drawing of pyramidal header

In this project, the geometry for the fluid flow needs to be simplified to improve the meshing time and simulation time. For the both of the header, the length of the outlet tube had been reduced from 127 mm to 1 mm only which is the optimum length for an acceptable amount of meshing and simulation time.

4.2 Meshing

Meshing is a very important step that need be completed before any CFD simulation can be performed. This is because in order to analyse the fluid flows the flow domains must be split into smaller subdomains which can be done by meshing. Since this project involves 3D geometry, there are six meshing methods available for 3D geometry which is tetrahedrons, sweep, multizone, hex dominant, cut cell mesh and automatic. However, for this project, tetrahedral mesh which involves patch conforming (TGrid based) and patch independent (ICEM CFD based) had been used as the meshing method. This is because, the tetrahedral mesh is the recommended meshing method when using FLUENT as the CFD simulation software.

Fig. 4.5 and Fig. 4.6 shows the geometry of semi cylindrical header and pyramidal header that had been meshed.

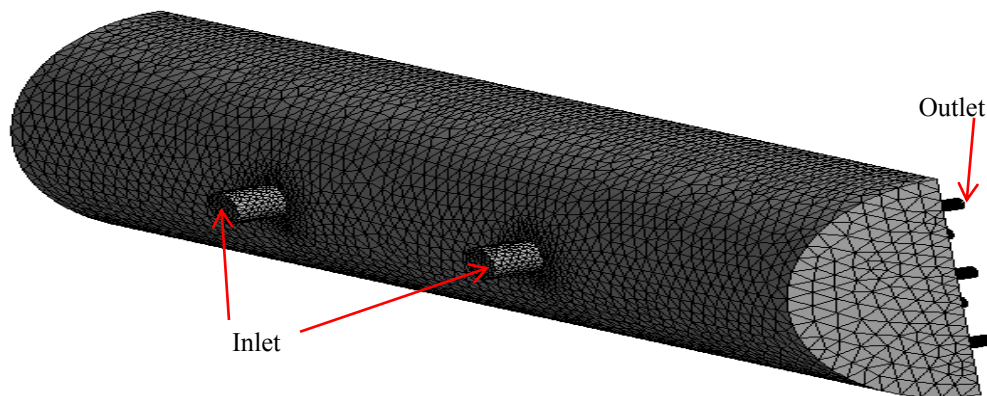


Figure 4.5: Semi cylindrical header that had been meshed

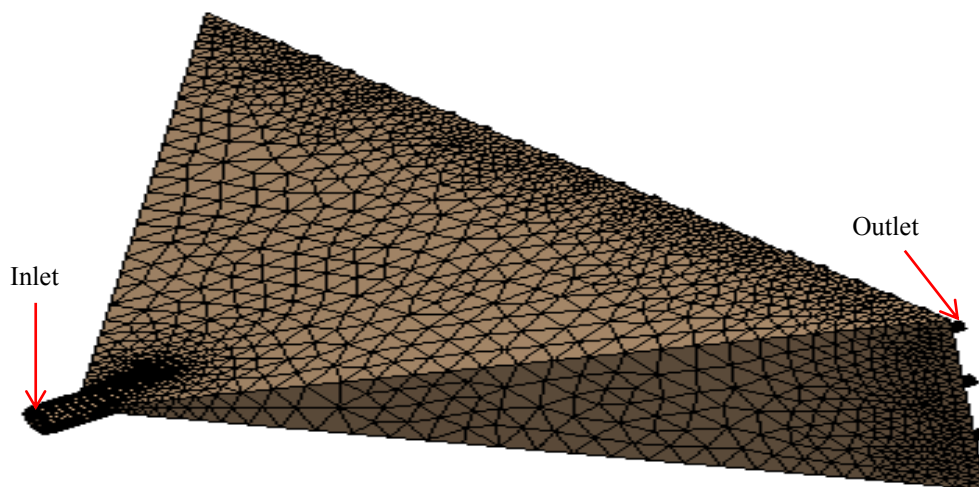


Figure 4.6: Pyramidal header that had been meshed

In Fig. 4.5 and Fig. 4.6, it can be clearly seen that tetrahedral mesh had been used as the meshing method for this geometry and there are also two surface selections that had been specified in this mesh which are inlet and outlet as shown in Fig. 4.4 and Fig. 4.5. In order to ensure that the meshing produce is within the accepted quality, the mesh statistics need to be check and Table 4.1 and Table 4.2 shows the mesh statistic for the semi cylindrical header and pyramidal header respectively.

Parameter		Value
Nodes		228936
Elements		1144358
Orthogonal Quality	Minimum	0.245
	Maximum	0.998
	Average	0.856
	Standard Deviation	0.085
Skewness	Minimum	8.470E-06
	Maximum	0.798
	Average	0.232
	Standard Deviation	0.122

Table 4.2: Mesh Statistic for Pyramidal Header

Parameter		Value
Nodes		226643
Elements		1130952
Orthogonal Quality	Minimum	0.234
	Maximum	0.998
	Average	0.856
	Standard Deviation	0.084
Skewness	Minimum	2.454E-5
	Maximum	0.800
	Average	0.233
	Standard Deviation	0.122

Based on the mesh statistics on Table 4.1 and Table 4.2, there are two parameters that will determine the quality of the mesh which are orthogonal quality and skewness. For orthogonal quality, the minimum value for semi cylindrical header and pyramidal header is 0.2448 and 0.234 respectively. For skewness, the maximum value for semi cylindrical header and pyramidal header is 0.798 and 0.8 respectively. Since both of the header had satisfied the minimum requirement for the two parameters which are minimum value for orthogonal quality must not be less than 0.05 and maximum value for skewness must not be greater than 0.9, the meshed geometry had an acceptable quality and can now be used in FLUENT for fluid flow analysis.

4.3 Scaled Residual

Scaled residual is one of the parameters that need to be monitored to determine the convergence of a solution. For this project, convergence criterion for scaled residuals had been set to default which is 10^{-6} for energy and 10^{-3} for other variables. Thus, the scaled residual for all the variables must be below or around the specified value in order for the solution to converge. Besides that, in order for the solution to converge, the scale residual for each of the variables must be constant or do not have significant amount of fluctuation. Fig. 4.7 and Fig. 4.8 shows the scaled residual of semi cylindrical header and pyramidal header fluid flow analysis for 1000 iterations.

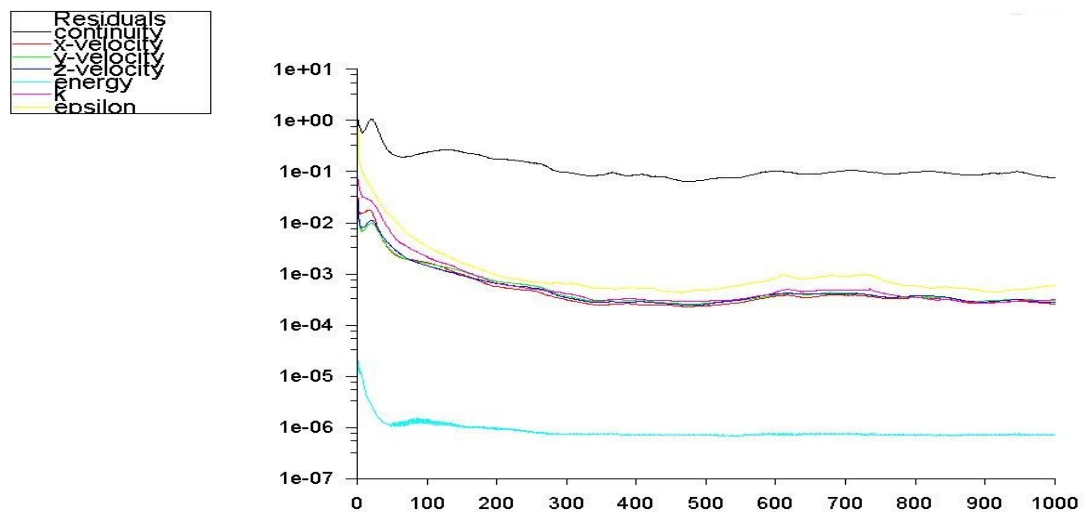


Figure 4.7: Scaled residual for semi cylindrical header fluid flow analysis

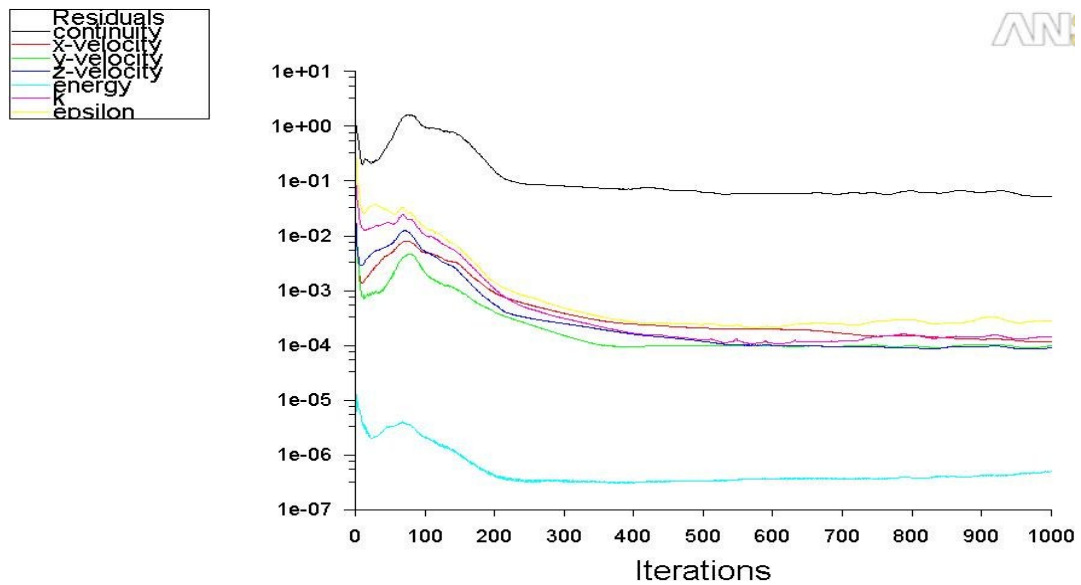


Figure 4.8: Scaled residual for pyramidal header fluid flow analysis

From Fig. 4.7 and Fig. 4.8, it can be clearly seen that most of the variables for both of the headers are able to satisfy the default convergence criterion set in this project whereby the scaled residual for x-velocity, y-velocity, z-velocity, K and epsilon are around 10^{-3} while the scaled residual for energy are around 10^{-6} . However, as for continuity, the scaled residual is around 10^{-1} which is higher than the default convergence criterion. This might be due to improper meshing which result in low mesh quality. Hence, the convergence criterion for continuity can be further decreased by improving the mesh quality of the header. However, due to time and technology constraint, this improvement cannot be made and thus, the current criterion for continuity had been accepted. Other than that, the scaled residual for all of the variables do not have significant amount of fluctuation and can be considered constant. Based on the analysis that had been done on scaled residual, it can be said the solution for both of the headers had converged but further analysis on temperature distribution and mass flow need to be done as an additional confirmation for solution convergence.

4.4 Mass Flow Report

Mass flow report had also been used to determine the convergence of a solution. In order for the solution to converge, the mass flow report must obey the principle of

mass conservation whereby the mass flow at the inlet flow must equal to the mass flow at the outlet. Table 4.3 shows the mass flow report for semi cylindrical header and pyramidal header.

Table 4.3: Mesh Statistic for Semi Cylindrical Header

Header	Surface	Mass flow rate (kg/s)
Semi Cylindrical	Inlet	0.001
	Outlet	0.0010000032
Pyramidal	Inlet	0.001
	Outlet	0.00099995821

From Table 4.3, it can be clearly seen that the difference between mass flow rate at the inlet and outlet is very small for both of the headers which is 3.23×10^{-9} for semi cylindrical header and 4.18×10^{-8} for pyramidal header. Since the difference is very small, it can be concluded that principle of mass conservation had been obeyed and the solution had converged.

4.5 Velocity Distribution

Velocity distribution is the most important parameter that needs to be measured since it can be used to calculate the relative and absolute flow maldistribution parameter which is denoted by S_i and S respectively. The relative flow maldistribution, S_i and absolute flow maldistribution, S can be calculated by using Eq. 16 and Eq. 17 respectively. Where N stands for number of tubes, $V_{ch(i)}$ stands for the velocity of each outlet tubes and V_{ave} stands for the average velocity of all the outlet tubes.

$$S_i = \frac{V_{ch(i)} - V_{ave}}{V_{ave}} \quad (16)$$

$$S = \sqrt{\frac{1}{N-1} \sum_{i=1}^N (V_{ch(i)} - V_{ave})^2} \quad (17)$$

Relative flow maldistribution parameter, S_i will determine how much the velocity at each of the outlet tubes deviates from the average velocity. Hence, the flow distribution for the MTS heat exchanger can be determined by analysing the difference in relative flow maldistribution between all the outlet tubes. The smaller the difference, the more uniform the flow distribution. However, in order to represent the flow maldistribution conditions under different header configuration parameters, a single value is needed and Eq. 17 can be used to calculate the required absolute flow maldistribution parameter, S which is a single value. Same like relative flow maldistribution, the smaller the absolute value, the more uniform the flow distribution will be.

4.5.1 Semi Cylindrical Header

Fig. 4.9 shows the contours for velocity at each of the outlet tubes whereby each tube had been assigned with unique number to represent the outlet tubes. Besides that, each outlet tubes had also been categorized into different rows ranging from row 1 until row 5.

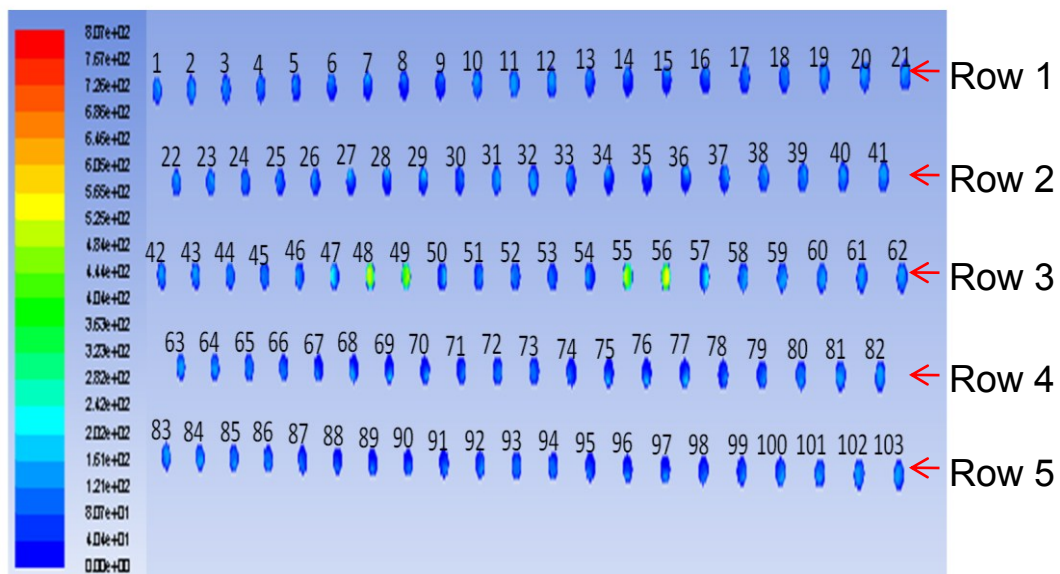


Figure 4.9: Contour of velocity at each of the outlet tubes

From Fig. 4.9, it can be clearly seen that there are 103 outlet tubes with tubes at row 3 has the highest velocity. This is because, the diameter for the inlet tube is very small compared to the dimension of the flow header. Hence, the fluid has higher tendency to go preferentially into the outlet tubes that are nearest whereby in this case are tubes at row 3. This situation can be further explained by analysing the velocity vector inside MTS heat exchanger as shown in Fig. 4.10.

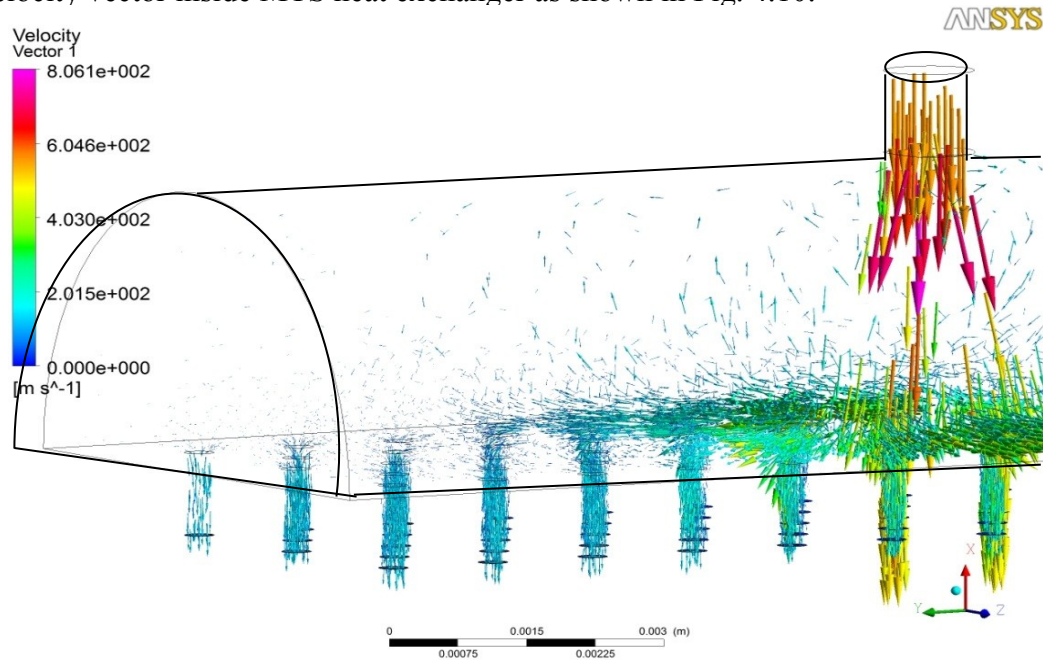


Figure 4.10: Velocity vector for half section of semi cylindrical header

Based on the data in Fig. 4.10, it had clearly explained the flow distribution inside the semi cylindrical header whereby most of the fluid had been distributed to the outlet tubes that directly facing the inlet tube which result in higher velocity at tube on row 3. On the other hand, the outlet tubes that are further away from the inlet tubes had less fluid flow especially the outlet tubes at the end of the header since the fluid had been distributed before it can reach the end of the header.

In order to determine the relative flow maldistribution parameter, S_i the velocity at each of the outlet tubes need to be determined and Fig. 4.11 shows the graph of velocity magnitude vs. serial number of outlet tubes

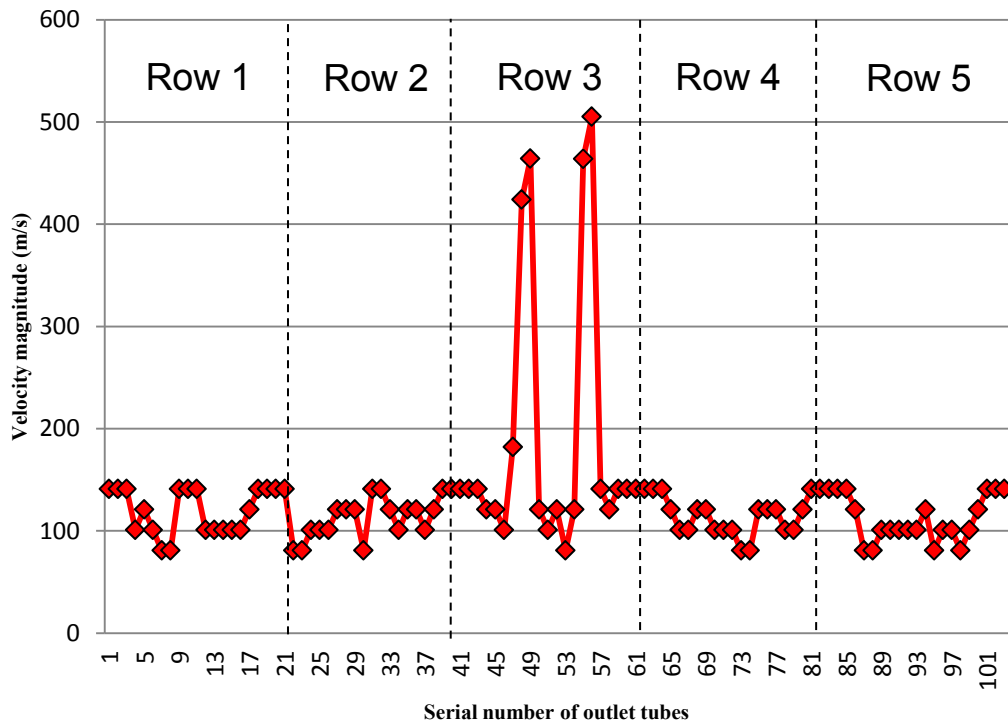


Figure 4.11: Velocity magnitude vs. serial number of outlet tubes

Based on Fig. 4.11, the maximum velocity is 500 m/s at tube 56 which is one of the outlet tubes in row 3. On the other hand, the minimum velocity is 80 m/s at tube 7, 8, 22, 23, 30, 73, 74, 87, 88, 95 and 98 which is actually the outlet tubes at row 1, row 2, row 4, and row 5. This is because, the outlet tube at these tubes are the furthest away from the inlet tubes. Hence, the results here once again prove that flow maldistribution occur in the semi cylindrical header and by using this data, the relative flow maldistribution for each of the outlet tubes can be calculated. Fig. 4.12 shows a graph of relative flow maldistribution parameter, S_i vs. serial number of outlet tubes.

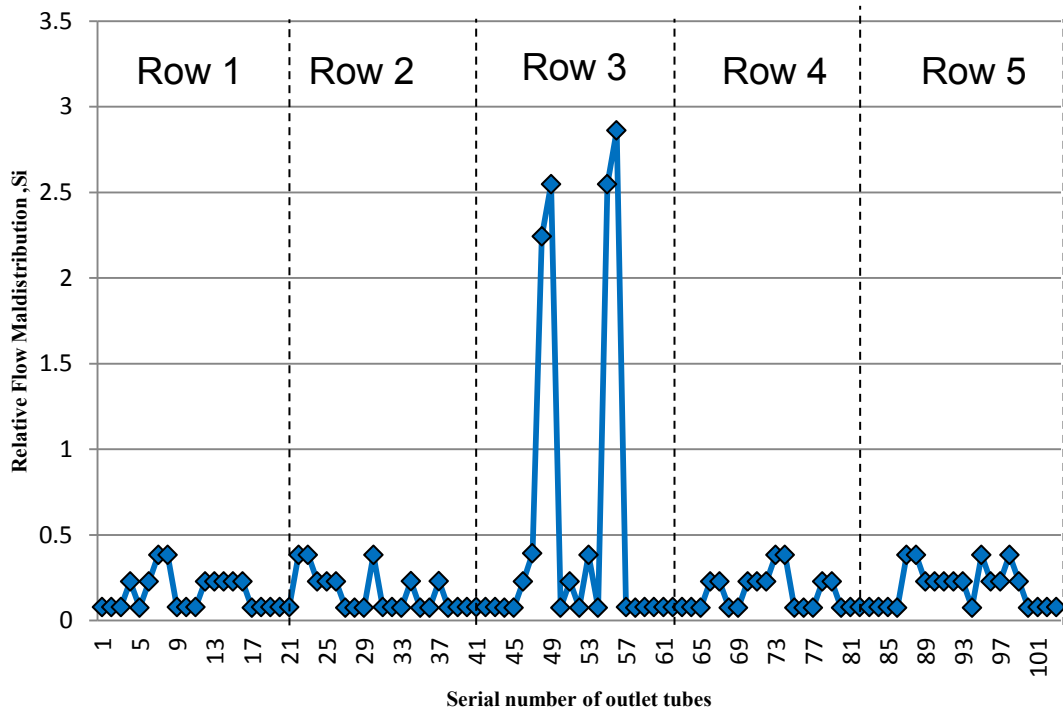


Figure 4.12: Relative flow maldistribution vs. serial number of outlet tubes

Based on the data from Fig. 4.12, it can be seen that there is a huge difference in the relative flow maldistribution for tube 48, 49, 55 and 56 which is the outlet tubes on row 3 that directly facing the inlet tubes. This is due to the large velocity magnitude at those outlet tubes compared to the other outlet tubes. As for absolute flow maldistribution, by using the data on Fig. 4.12, the absolute flow maldistribution for semi cylindrical header is equal to 70. Hence, based on the relative and absolute flow maldistribution, it can be said that the flow maldistribution for semi cylindrical header is very serious and necessary improvement on the header configuration need to made to decrease the effect of flow maldistribution.

4.5.2 Pyramidal Header

Fig. 4.13 shows the contours for velocity at each of the outlet tubes whereby each tube had been assigned with unique number to represent the outlet tubes. Besides that, each outlet tubes had also been categorized into different rows ranging from row 1 until row 5.

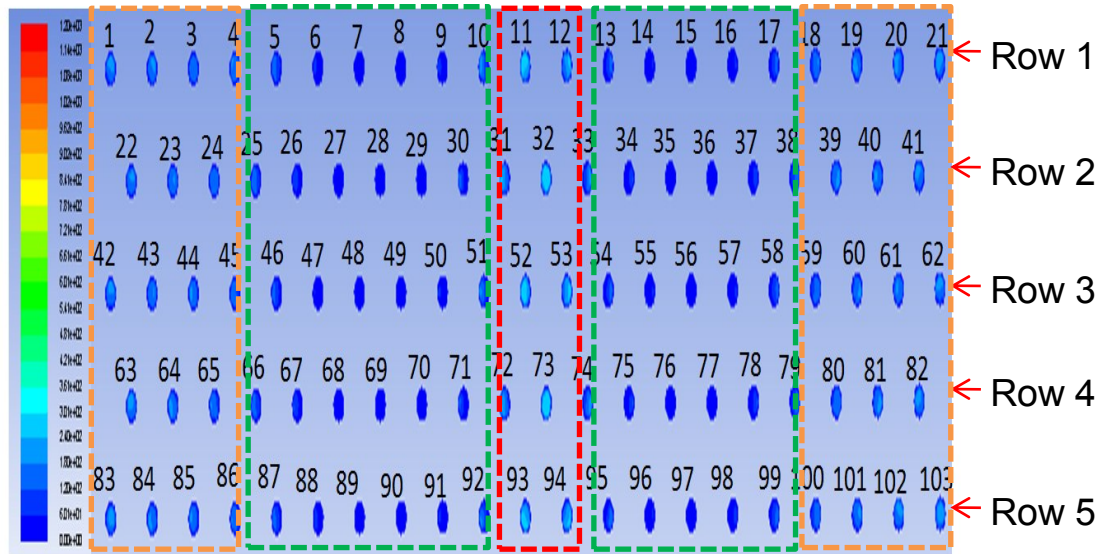


Figure 4.13: Contour of velocity at each of the outlet tubes (m/s)

From Fig. 4.13, it can be clearly seen that there are three regions separating the outlet tubes according to velocity. Region 1 which is denoted by red lines has the highest velocity followed by region 3 which is denoted by orange lines and lastly is region 2 which is denoted by green lines. This behaviour of fluid velocity can be explained by studying the velocity vector as shown in Fig. 4.14.

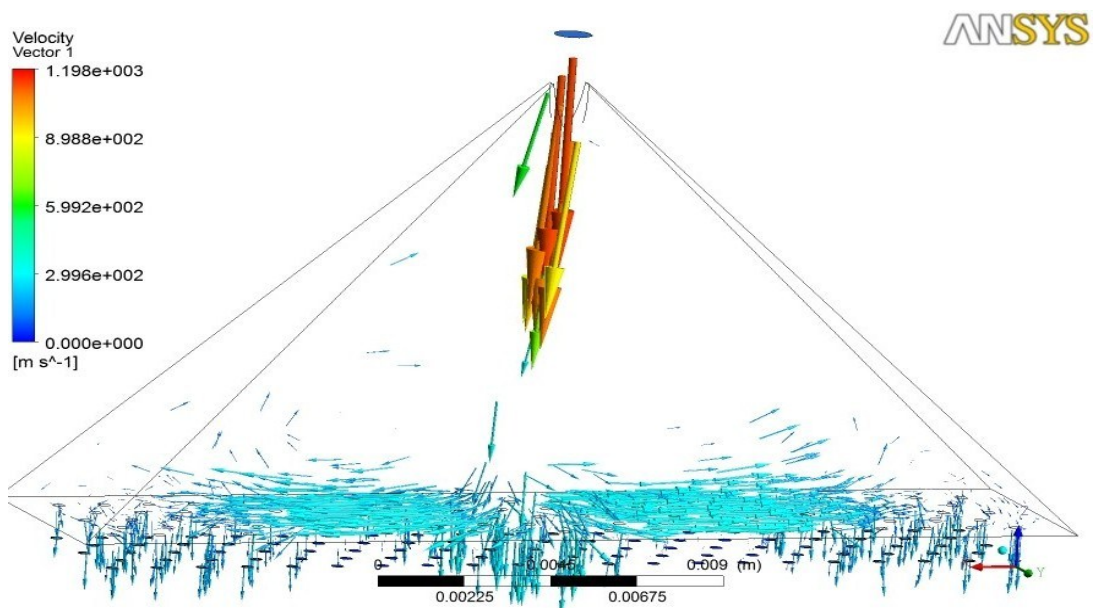


Figure 4.14: Velocity vector for pyramidal header

From Fig. 4.14, it can be clearly seen that the velocity vector flow preferentially to the centre of the header which is in this case is the middle outlet tubes in every rows and thus, the outlet tubes on this region has the highest velocity. However, for pyramidal header, the outlet tubes in region 3 which is at the end of the header has

higher velocity compare to outlet tubes in region 3 which is much closer to the inlet tube. This behaviour is actually the opposite of what had happened for semi cylindrical header and might be due to pyramidal header has higher height than semi cylindrical header. As a result, the fluid will dispersed too fast and there is insufficient time for the fluid to flow into respective outlet tubes especially on region 2. However, once the fluid reach region 3, the dispersion become slower and the fluid will have sufficient time to settle in to the outlet tubes.

In order to determine the relative flow maldistribution parameter, S_i the velocity at each of the outlet tubes need to be determined and Fig. 4.15 show the graph of velocity magnitude vs. serial number of outlet tubes for pyramidal header

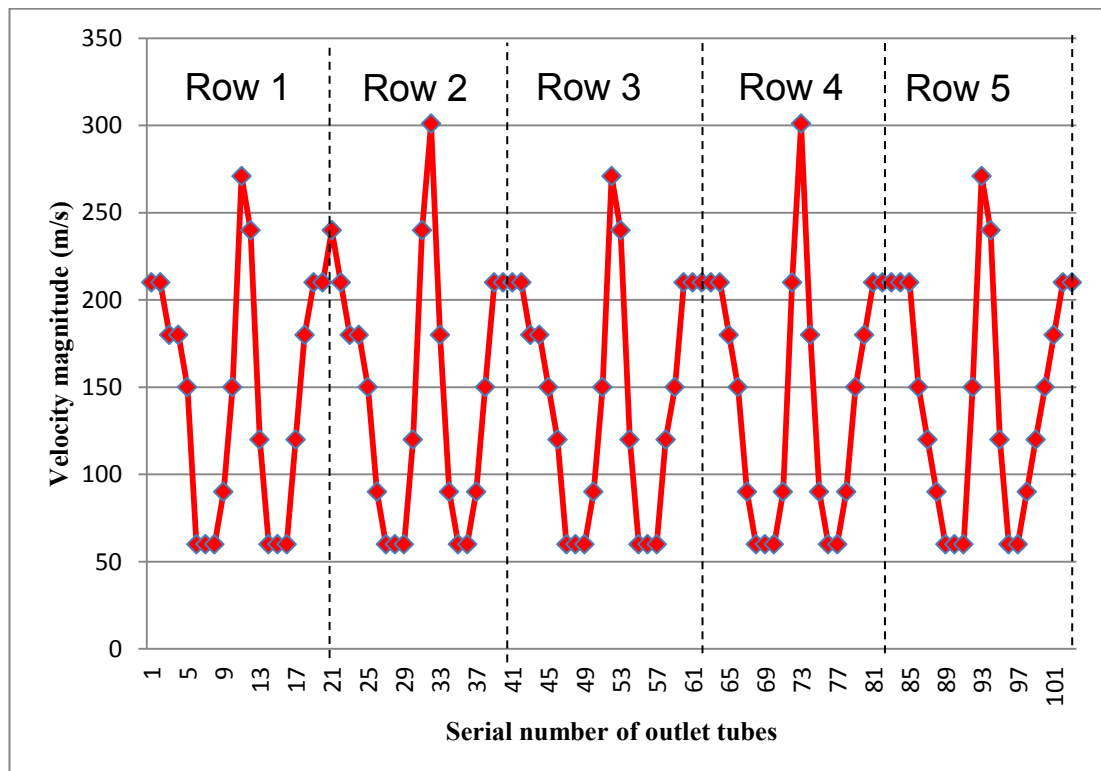


Figure 4.15: Velocity magnitude (m/s) vs serial number of outlet tubes

From Fig. 4.15, the maximum velocity is 300 m/s while the minimum velocity is 60 m/s. Pyramidal header has lower maximum and minimum velocity than semi cylindrical header because it has higher header height than semi cylindrical header. As a result, the rate of dispersion is higher in pyramidal header than semi cylindrical header. The data from Fig. 4.15 can be used to calculate the relative and absolute flow maldistribution parameter and Fig. 4.16 shows the relative flow maldistribution parameter for pyramidal header.

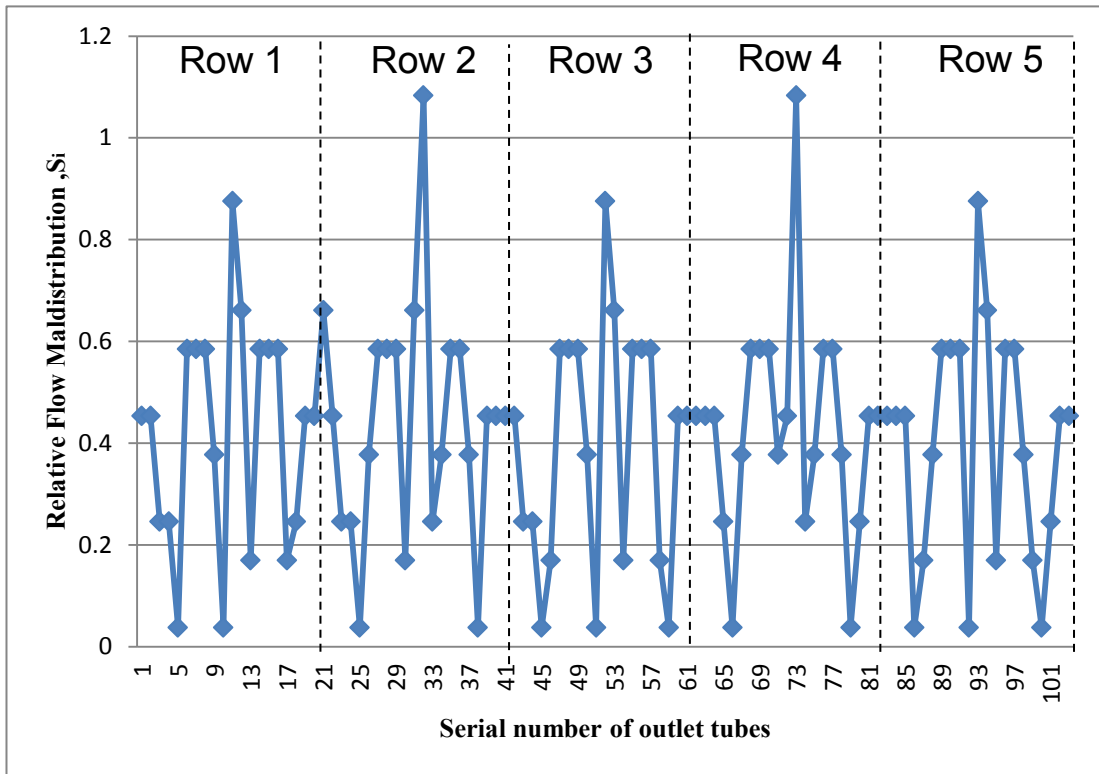


Figure 4.15: Relative flow maldistribution parameter for pyramidal header

Based on the data from Fig. 4.15, it can be clearly seen that highest relative flow maldistribution parameter for pyramidal header is 1.1 which is much less than relative flow maldistribution parameter for semi cylindrical header. However, the severity between these two header are still cannot be compare because the relative flow maldistribution for semi cylindrical header is more uniform than relative flow maldistribution for pyramidal header. Thus, in order to determine the severity of flow maldistribution and decide which header is the best to reduce the effect of flow maldistribution, absolute flow maldistribution parameter must be calculated. The absolute flow maldistribution for pyramidal header is 60 which is less than absolute flow maldistribution for semi cylindrical header. Even though the difference is small but pyramidal header prove to be better in reducing the effect of flow maldistribution in MTS heat exchanger than semi cylindrical header.

4.6 Temperature Distribution

Other than scaled residual and mass flow report, temperature distribution had also been used to determine the convergence of a solution. This is being done by comparing the simulation data with the experimental data whereby ideally, the tube side outlet temperature for the simulation must be equal or close to the experimental data. Based on the experimental data on Table 2.1, the tube side outlet temperature for 0.001 kg/s of nitrogen is around 331 K. However, that data is obtained by using 3 modules of MTS heat exchanger arranged in parallel with each other. On the other hand, the simulation is being done only on the inlet header for one module of MTS heat exchanger. Hence, the solution is acceptable and can be considered to converge as long as the tube outlet temperature does not exceed 331 K

4.6.1 Semi Cylindrical Header

Fig. 4.16 shows the contours for temperature at each of the outlet tubes whereby each tube had been assigned with unique number to represent the outlet tubes. Besides that, the outlet tubes had also been divided into 5 different rows ranging from row 1 until row 5.

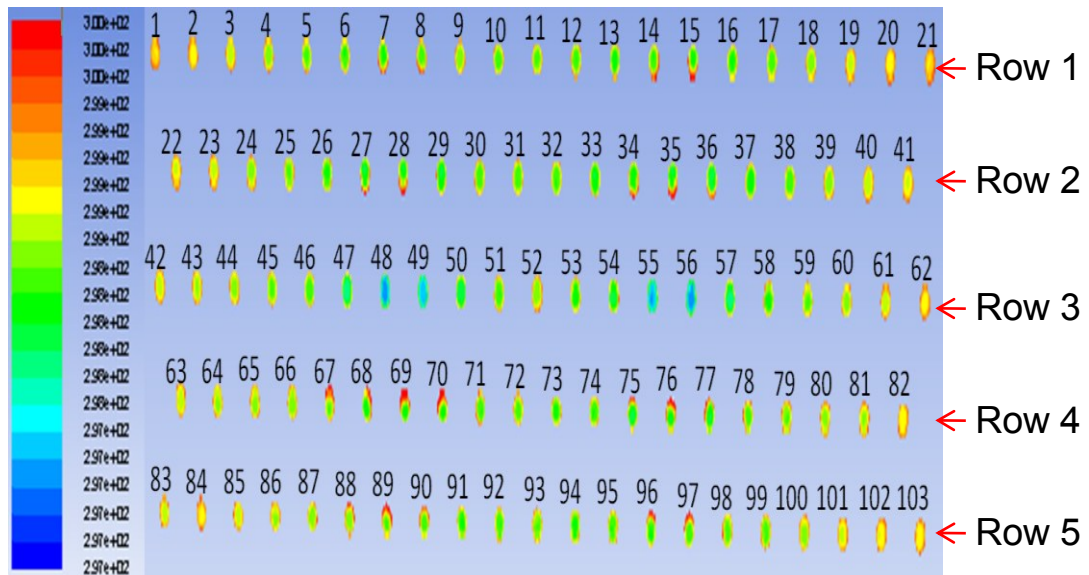


Figure 4.16: Contour for temperature (K) at each outlet tubes for semi cylindrical header

Based on Fig. 4.16, it can be clearly seen that row 3 has the outlet tubes with the lowest temperature which is tube 48, 49, 55 and 56 while the highest temperature is at the outlet tubes situated at the end of the header. This is because, the fluid flow

velocity in tube 48, 49, 55 and 56 is the highest and thus there will be insufficient time for heat transfer between shell side fluid and tube side fluid to take place. The same can also be said to the other outlet tubes but vice versa.

Graphical representation can be used to observe the relationship between outlet tubes and temperature whereby Figure 4.17 shows the line graph of temperature vs. serial number of outlet tubes.

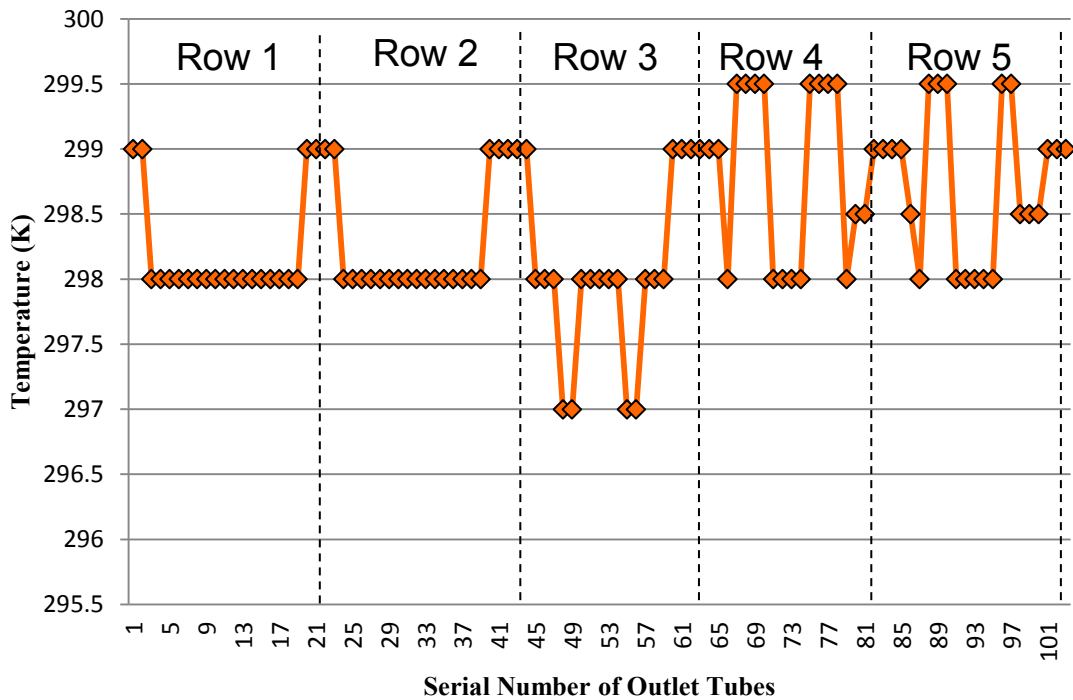


Figure 4.17: Temperature (K) vs. serial number of outlet tubes for semi cylindrical header

In Fig. 4.17, the temperature distribution had also been divided into the same region like in Fig. 4.6 whereby tubes 48, 49, 55 and 56 has the lowest temperature which is 297 K. On the other hand, outlet tubes on row 4 and row 5 has the highest temperature which is 299.5 K while the highest temperature for row 1 and row 2 is 299 K. Row 1, 2, 4 and 5 has higher temperature than row 3 because these rows has lower velocity than row 3

4.6.1 Pyramidal Header

Fig. 4.18 shows the contours for temperature at each of the outlet tubes whereby each tube had been assigned with unique number to represent the outlet tubes. Besides that, the outlet tubes had also been divided into 5 different rows ranging from row 1 until row 5

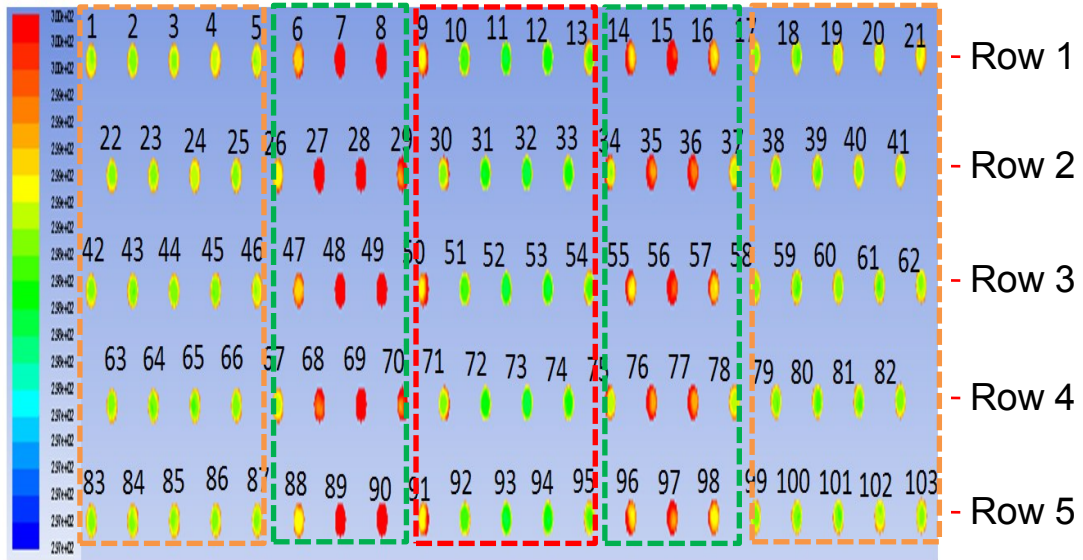


Figure 4.18: Contour for temperature (K) at each outlet tubes for pyramidal header

For pyramidal header, the temperature distribution at outlet tubes can be divided into 3 regions according to the degree of hotness whereby region 1 which is denoted by red lines has the lowest temperature. On the other hand, region 2 which is denoted by green lines has the highest temperature followed by region 3 which is denoted by orange lines. This temperature pattern exists due to the different fluid flow velocity in each region whereby region 2 has the lowest velocity followed by region 3 and finally region 1. Higher velocity means that there will be insufficient time for heat transfer between shell side fluid and tube side fluid to take place.

Fig. 4.19 shows the line graph of temperature vs. serial number of outlet tubes for pyramidal header which had also been divided into 5 rows of outlet tubes.

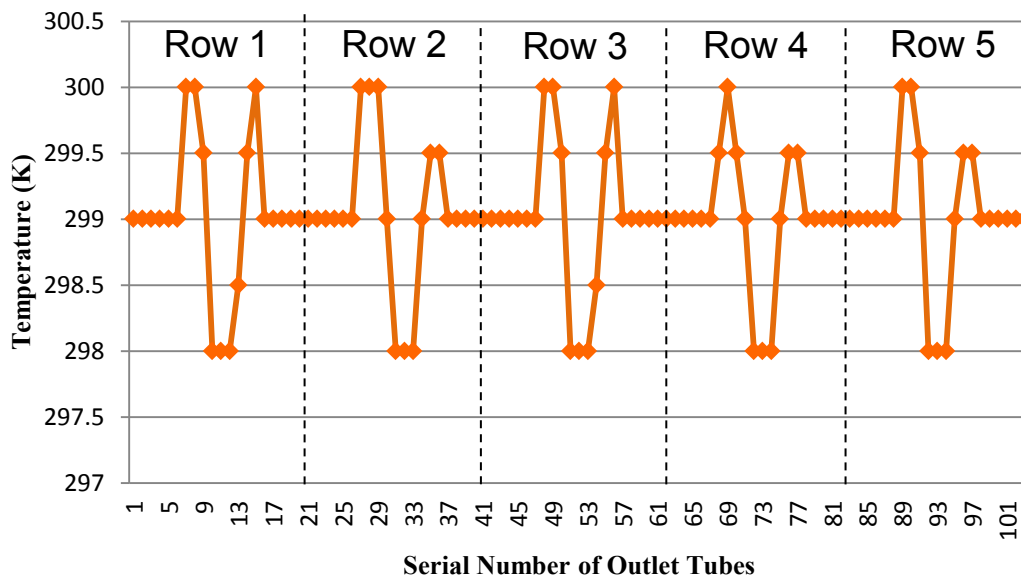


Figure 4.19: Temperature (K) vs. serial number of outlet tubes for pyramidal header

In Fig. 4.19, the maximum temperature is 300K while the minimum temperature is 298K. Both the maximum and minimum temperature for pyramidal header is higher than semi cylindrical header because the maximum and minimum velocity in pyramidal header is lower than in semi cylindrical header.

4.7 Discussion

4.7.1 Comparison on Relative Flow Maldistribution Parameter

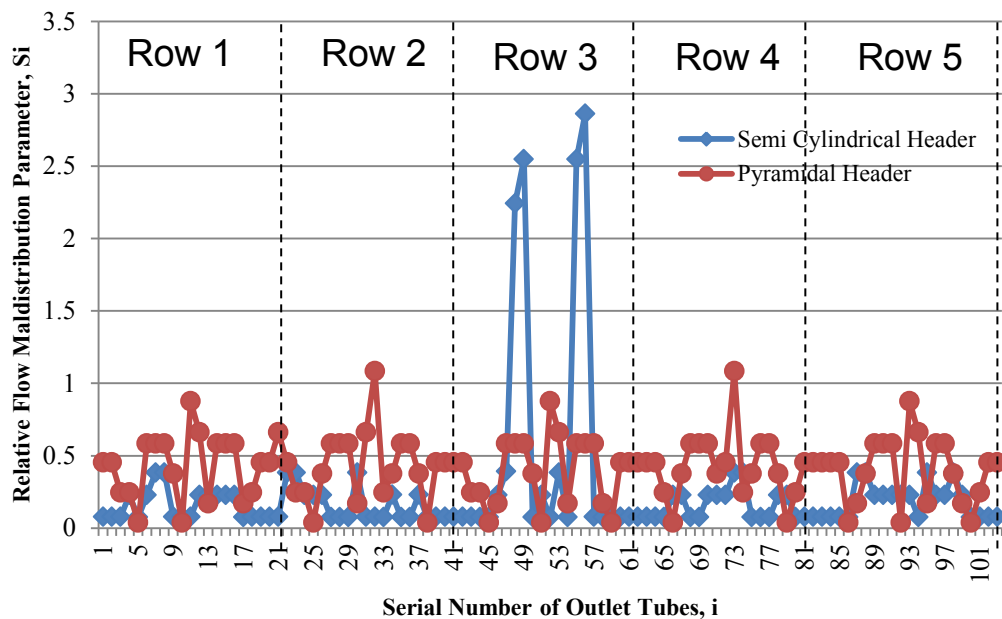


Figure 4.20: Comparison on relative flow maldistribution parameter between semi cylindrical header and pyramidal header

Fig. 4.20 shows the comparison on relative flow maldistribution parameter between semi cylindrical header and pyramidal header. From Fig. 4.20, it can be clearly seen that the maximum relative flow maldistribution parameter for semi cylindrical header is higher than for pyramidal header. However, in term of deviation between the outlet tubes, semi cylindrical header has smaller deviation than pyramidal header. As a result, the absolute flow maldistribution parameter in pyramidal header is 60 while in semi cylindrical header is 70. Even though the difference in absolute flow maldistribution parameter between semi cylindrical header and pyramidal header is small but since the absolute flow maldistribution parameter in pyramidal header is lower than in semi cylindrical header, then pyramidal header is better in reducing the severity of flow maldistribution.

4.7.2 Comparison on Temperature Distribution

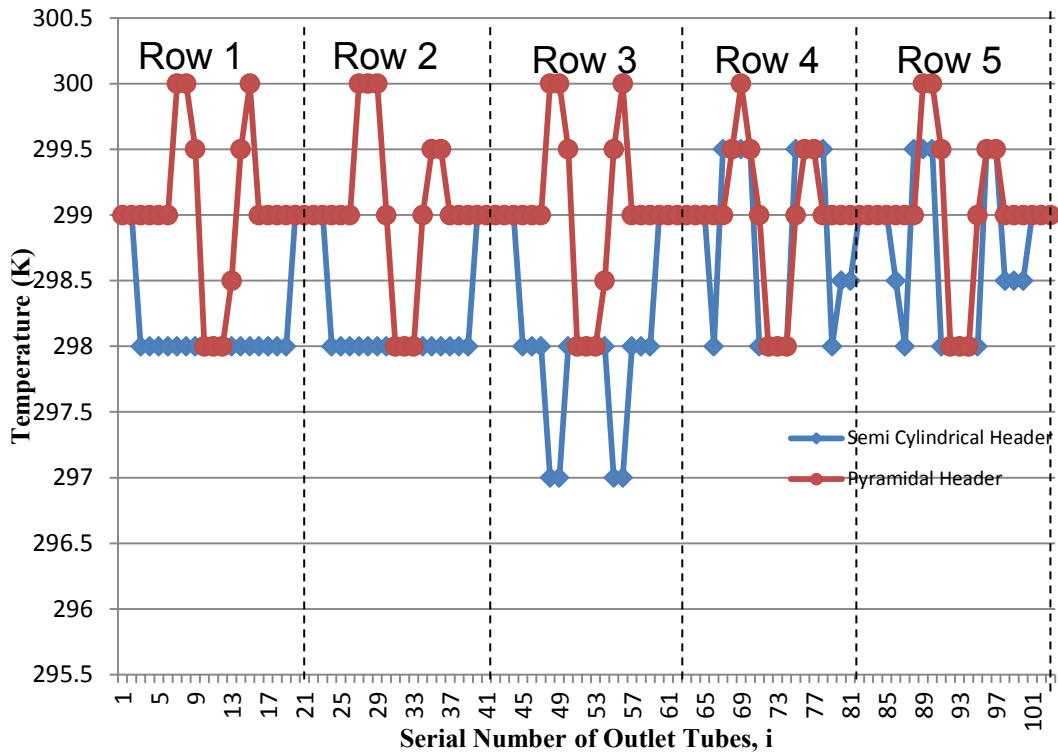


Figure 4.21: Comparison on temperature (K) between semi cylindrical header and pyramidal header

Fig. 4.21 shows the comparison on temperature (K) between semi cylindrical header and pyramidal header. From Fig. 4.21, pyramidal header has higher maximum and minimum temperature than semi cylindrical header. This is because, pyramidal header has lower maximum and minimum velocity than semi cylindrical header. As a result, there is more time for heat transfer between shell side fluid and tube side fluid in pyramidal header than in semi cylindrical header.

4.7.3 Validation

In order to validate the simulation data, the temperature distribution can be compared with experimental data. Table 4.4 shows the experimental data for a complete prototype of MTS heat exchanger that consist of 3 modules and using semi cylindrical header that had been taken from previous research paper.

Table 4.4: Experimental Data for a Complete Prototype of MTS Heat Exchanger

\dot{m} (mg/s)	p (kPa)	T_1 (C)	T_2 (C)	T_3 (C)	T_4 (C)	ϵ (%)	NTU	UA (W/K)	UA [Eq. (5)]
Nitrogen									
470 ± 20	322 ± 3	104.7 ± 0.5	30.9 ± 0.5	23.0 ± 0.5	93.0 ± 0.5	85.7 ± 0.6	6.0 ± 0.3	3.7 ± 0.4	7.1
840 ± 20	322 ± 3	96.5 ± 0.5	32.3 ± 0.4	23.3 ± 0.5	84.1 ± 0.5	83.1 ± 0.7	4.9 ± 0.2	5.3 ± 0.5	7.1
930 ± 20	322 ± 3	99.4 ± 0.5	33.0 ± 0.5	22.8 ± 0.5	85.8 ± 0.5	8.2 ± 0.7	4.6 ± 0.2	5.4 ± 0.5	7.1
373 ± 20	705 ± 3	51.4 ± 0.5	28.5 ± 0.5	26.1 ± 0.5	48.8 ± 0.5	89.7 ± 0.7	8.7 ± 0.6	3.5 ± 1.4	7.1
738 ± 20	1462 ± 3	64.7 ± 0.5	28.9 ± 0.5	25.3 ± 0.5	59.2 ± 0.5	86.0 ± 0.7	6.1 ± 0.4	6.0 ± 1.3	7.1
1085 ± 20	1068 ± 3	64.8 ± 0.5	28.6 ± 0.5	23.6 ± 0.5	58.3 ± 0.5	84.2 ± 0.7	5.3 ± 0.3	7.1 ± 1.2	7.1
1413 ± 20	1486 ± 3	67.3 ± 0.5	29.3 ± 0.5	22.9 ± 0.5	59.5 ± 0.5	82.4 ± 0.7	4.7 ± 0.2	7.9 ± 1.1	7.1
1824 ± 20	1470 ± 3	58.1 ± 0.5	23.3 ± 0.5	15.3 ± 0.5	48.8 ± 0.5	78.2 ± 0.7	3.6 ± 0.1	7.6 ± 0.9	7.1
Helium									
117 ± 7	749 ± 3	107.5 ± 0.5	28.3 ± 0.5	23.5 ± 0.5	103.6 ± 0.5	95.4 ± 0.6	21 ± 3	11.1 ± 2.5	39.0
79 ± 7	756 ± 3	103.8 ± 0.5	29.5 ± 0.5	24.0 ± 0.5	100.5 ± 0.5	95.7 ± 0.7	22 ± 4	6.9 ± 1.6	39.0
213 ± 7	825 ± 3	109.4 ± 0.5	28.7 ± 0.5	23.1 ± 0.5	103.4 ± 0.5	93.0 ± 0.7	13.3 ± 1.4	15.4 ± 2.6	39.0

In Table 4.4, T_1 and T_2 are the shell side inlet and outlet temperature respectively while T_3 and T_4 are the tube side inlet and outlet temperature respectively. Besides that, the red line in Table 4.4 shows the part of the experimental data that had been chosen as a comparison with the simulation data.

For the simulation, only the inlet semi cylindrical header for one module of MTS heat exchanger had been used. Hence, there is a need for heat transfer correlation to be used in order to calculate the outlet tube side temperature for before the data can be validated. Eq. 18 shows the heat transfer equation used to calculate the amount of heat that need to be transferred from the shell side while Eq. 19 shows the heat transfer equation used to calculate the tube side outlet temperature for 3 module of MTS heat exchanger based on inlet temperature from simulation data.

$$q = mCp(T_1 - T_2) \quad (18)$$

$$q = snk \frac{2\pi L(r_2 - r_1)}{\ln(r_2 / r_1)} \frac{T_4 - T_3}{r_2 - r_1} \quad (19)$$

Whereby

- q : Heat that need to be transferred from shell side fluid
- m : Mass flow rate of shell side fluid
- Cp : Specific heat capacity for shell side fluid
- n : Number of tubes
- k : Thermal conductivity of tube
- L : Length of tube
- s : No. of module
- r_2 : Outer radius
- r_1 : Inner radius
- T_1 : Shell side inlet temperature (experimental)
- T_2 : Shell side outlet temperature (experimental)

- T_3 : Tube side inlet temperature (simulation)
 T_4 : Tube side outlet temperature (simulation)

By using Eq. 18, the amount of heat that needs to be transferred from the shell side fluid is 37.4 W. On the other hand, by using Eq. 19, the tube side outlet temperature for one module of MTS heat exchanger is 301 K while from experimental data, the tube side outlet temperature is 331 K. Hence there is 9% difference in the tube side outlet temperature between the simulation and experimental data. Since the difference is small, the simulation data is acceptable and reliable.

CHAPTER 5

CONCLUSION AND RECOMMENDATION

5.1 Conclusion

Simulation on the fluid flow for both semi cylindrical header and pyramidal header of MTS heat exchanger had been done using ANSYS FLUENT. Besides that, in term of validation, the temperature distribution for semi cylindrical header shows only small difference with the experimental data which suggest that the simulation data is acceptable and reliable. Based on the velocity distribution data from simulation pyramidal header is relatively better than semi cylindrical header in term of reducing the flow maldistribution inside MTS heat exchanger. This is because, the absolute flow maldistribution parameter for pyramidal header is less than for semi cylindrical header which suggest that the flow distribution is more uniform in pyramidal header than in semi cylindrical header.

5.1 Recommendation

For future work, it is recommended to use constructal distributor as the distributor configuration for MTS heat exchanger. This is because, unlike conventional distributor, there will be less pressure drop by using constructal distributor. Besides that, there might also be some advantages in term of pressure drop and efficiency by using two different headers configuration for the inlet and outlet. Other than that, it is also recommended to conduct the numerical modelling and simulation of MTS heat exchanger based on its application for engine cooling system in F1 car

CHAPTER 6

REFERENCES

- [1] F.D. Doty. "Microtube-strip heat exchanger" U.S. Patent 4 676 305, Jun. 30, 1987
- [2] F.D. Doty, G. Hosford and J.B. Spitzmesser. (1991). The microtube strip heat exchanger. *Heat Transfer Engineering* [Online]. 12(3), 31-41. Available: http://www.198.173.87.9/PDF/1991_HTE_Doty_HeatExchanger.pdf
- [3] A. Shirzadi, E. R. Wallach. (2004). New method to diffusion bond superalloys. *Science and Technology of Welding and Joining* [Online]. 9, 37-40. Available: <http://www.msm.cam.ac.uk/phase-trans/2005/Amir/p37.pdf>
- [4] K. Lange, K.Pohlandt, *Handbook of Metal Forming*. McGraw Hill, New York, 1985.
- [5] S. Kakac and H. Liu, "Basic design methods of heat exchangers, " in *Heat Exchangers Selection, Rating, and Thermal Design*, 2nd ed. Florida: CRC , 2002, ch. 2, sec. 6, pp. 57-60.
- [6] A. C. Mueller and J. P. Chiou. (1988). Review of various types of flow maldistribution in heat exchanger. *Heat Transfer Engineering* [Online]. 9(2), 36-49. Available:<http://www.tandfonline.com/doi/abs/10.1080/01457638808939664>
- [7] L. Luo, Y. Fan, W. Zhang, X. Yuan and N. Midoux. (2007, Feb.). Integration of constructal distributors to a mini crossflow heat exchanger and their assembly configuration optimization. *Chemical Engineering Science*[Online]. 62(13),. Available: <http://www.sciencedirect.com/science/article/pii/S0009250907002825>
- [8] S. Lalot, P. Florent, S.K. Lang and A.E. Bergles. (1999, Aug.). Flow maldistribution in heat exchangers. *Applied Thermal Engineering* [Online]. 19(8), 847-863. Available: <http://www.sciencedirect.com/science/article/pii/S1359431198000908>
- [9] A. Jiao, R. Zhang and S. Jeong. (2003, July). Experimental investigation of header configuration on flow maldistribution in plate-fin heat exchanger. *Applied Thermal Engineering* [Online]. 23(10), 1235-1246. Available: <http://www.sciencedirect.com/science/article/pii/S1359431103000577>
- [10] A. Bejan. (1997, March). Constructal-theory network of conducting paths for cooling a heat generating volume. *International Journal of Heat and Mass Transfer* [Online]. 40(4), 799-811. Available: <http://www.sciencedirect.com/science/article/pii/0017931096001755>

